

01-0004343

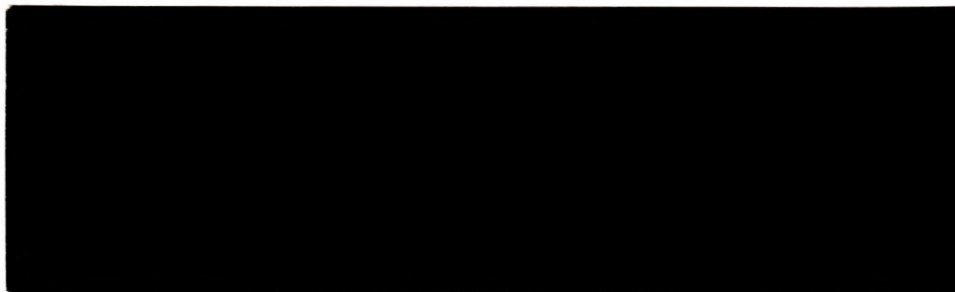
# CANMET

Canada Centre for  
Mineral and Energy  
Technology

Centre canadien de la  
technologie des  
minéraux et de l'énergie

**Mining  
Research  
Laboratories**

**Laboratoires  
de recherche  
minière**



DECLASSIFIED  
Jan 8 19 93  
by Mona Hamel  
for  
Heer Larsoque

MRL (DECLASSIFIED)  
MRL 87-094 (TR) e.2

MRL 87-094 (TR) e.2



Energy, Mines and  
Resources Canada

Énergie, Mines et  
Ressources Canada

Canada

THE ENERGY OF OUR RESOURCES - THE POWER OF OUR IDEAS

L'ÉNERGIE DE NOS RESSOURCES - NOTRE FORCE CRÉATRICE



Canmet Information  
Centre  
D'information de Canmet

JAN 27 1997

555, rue Booth ST.  
Ottawa, Ontario K1A 0G1

1-4340

1-4343

GEOTECHNICAL STUDIES AT EAST BULL LAKE RESEARCH AREA  
(RA-7) *c-2*

*CRUB*

EDITED BY: A.G. Latham  
Geomagnetic Laboratory,  
Geological Survey of Canada

MRL 87-94 (~~INT~~) TR

June 1987

<p>DECLASSIFIED</p> <p><i>Jan 8 19 93</i></p> <p><i>as per</i></p> <p><i>Glen Larocque</i></p>
--

7-4343e2  
CPUB

NUCLEAR FUEL WASTE MANAGEMENT PROGRAM

GEOTECHNICAL STUDIES AT EAST BULL LAKE RESEARCH AREA (RA-7)

ROCK PROPERTIES

Edited by

A.G. Latham

Geomagnetic Laboratory

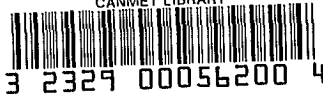
Geological Survey of Canada

601 Booth Street

Ottawa, Ontario

K1A 0E8

CANMET LIBRARY



C 2.  
CPUB

June 1987

ADDRESSES AND AFFILIATIONS OF AUTHORS AND EDITORS

A. Annor  
R. Jackson (AECL Secondment)  
Energy, Mines and Resources Canada  
Canada Centre for Mineral and Energy Technology (CANMET)  
555 Booth Street  
OTTAWA, Ontario  
K1A 0G1

P.J. Chernis (AECL Secondment)  
M.J. Drury  
P.B. Robertson  
Energy, Mines and Resources Canada  
Geological Survey of Canada  
1 Observatory Crescent  
OTTAWA, Ontario  
K1A 0Y3

K.L. Harding (AECL Secondment)  
P. Lapointe  
A.G. Latham  
Energy, Mines and Resources Canada  
Geological Survey of Canada  
Geomagnetic Laboratory  
601 Booth Street  
OTTAWA, Ontario  
K1A 0E8

J.P. Hume (AECL Secondment)  
T.J. Katsube  
J.B. Percival (AECL Secondment)  
Energy, Mines and Resources Canada  
Geological Survey of Canada  
601 Booth Street  
OTTAWA, Ontario  
K1A 0E8

W.A. Morris  
Morris Magnetics  
RR#2  
LUCAN, Ontario  
MON 2J0

TABLE OF CONTENTS

	<u>PAGE</u>
CHAPTER 1: INTRODUCTION AND DIGEST	3
A.G. Latham	
CHAPTER 2: GEOLOGY	7
2.1 <u>GENERAL GEOLOGY OF THE EAST BULL LAKE LAYERED COMPLEX</u>	9
P.J. Chernis and P.B. Robertson	
2.2 <u>PORE - MICROCRACK STRUCTURES</u>	17
P.J. Chernis	
CHAPTER 3: PHYSICAL PROPERTIES	29
3.1 <u>MECHANICAL PROPERTIES</u>	31
A. Annor and R. Jackson	
3.2 <u>PORE STRUCTURE CHARACTERISTICS</u>	39
J.P. Hume and T.J. Katsube	
3.3. <u>THERMAL PROPERTIES</u>	67
M. Drury	
CHAPTER 4: GEOPHYSICAL PROPERTIES	75
4.1 <u>MAGNETIC PROPERTIES</u>	77
A.G. Latham, W.A. Morris, P. Lapointe and K.L. Harding	
CHAPTER 5: EVALUATION OF ROCK PROPERTIES	97
A.G. Latham	
5.1 <u>DIGEST</u>	99
5.2 <u>DISTRIBUTION AND RANGES OF VALUES</u>	100
5.3 <u>ASSESSMENT OF VALUES</u>	102
CHAPTER 6: CONCLUSIONS & RECOMMENDATIONS	105
A.G. Latham	

CHAPTER 1

INTRODUCTION AND DIGEST





A.G. Latham  
Geomagnetic Laboratory  
Geological Survey of Canada  
601 Booth street  
Ottawa, Ontario  
K1A 0E8

The nuclear fuel waste disposal concept chosen for assessment in Canada involves the isolation of corrosion-resistant containers of waste in a vault located deep in plutonic rock. Acceptance or rejection of the concept therefore, requires the capability of assessing the long-term performance of the disposal system. Among the multiple barriers in which the corrosion-resistant containers will be placed, the host rock, the final barrier, is currently considered to be the most important. Therefore, it is necessary to evaluate extensively the long-term stability of the rock surrounding the vault, the effects of excavation, and of its radionuclide containment capacity.

The vault is currently chosen to be at a depth of approximately 1000 metres, so the vertical and horizontal stresses will be high. The heat from the spent fuel is expected to raise the temperature of the vault walls and the surrounding host rock for a certain period of time. The existing hydraulic gradient will have to be estimated in its magnitude and configuration, and this is expected to be perturbed by a thermo-hydraulic gradient due to the heat of the spent fuel. There will be a radionuclide concentration gradient between the vault and the

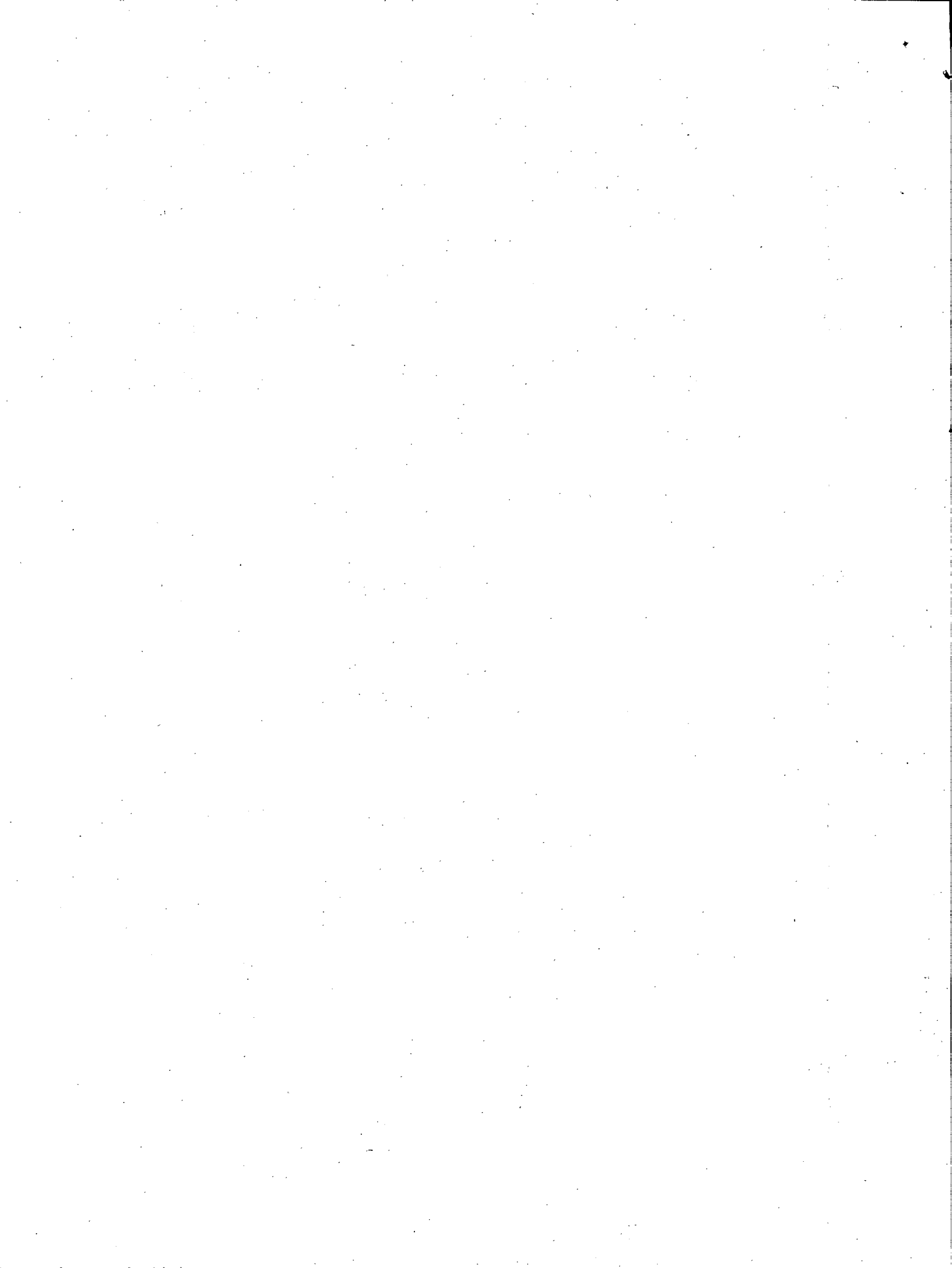
host rock if containment canisters, backfill, and buffer materials fail. Diffusion rates must be computed in order to estimate this contribution to nuclide transport.

The assessment and prediction of vault viability is affected by extensive modelling, in which values for the various physical rock properties of the matrix are input to the models. The petro-physical properties of concern are; the strength, elastic modulus, Poisson's ratio, thermal conductivity, thermal diffusivity, coefficient of linear thermal expansion, porosity, permeability and formation factor. These properties vary from pluton to pluton, and for various lithologies within a pluton. It is therefore, imperative to study these physical properties at ambient and at elevated temperatures, on the laboratory scale and on a field-macroscopic scale.

The study of magnetic properties plays a rather different role in rock property evaluation of the vault environment. Whereas hydraulic, thermal and mechanical studies are directly concerned with vault integrity, leakage aspects, etc., on micro- and meso-scales, magnetic studies are related more to overall lithology and alteration of the whole rock body. They contain nearfield, borehole specific properties, and in the case of granites, are directly related to the history of fracture-induced alteration.

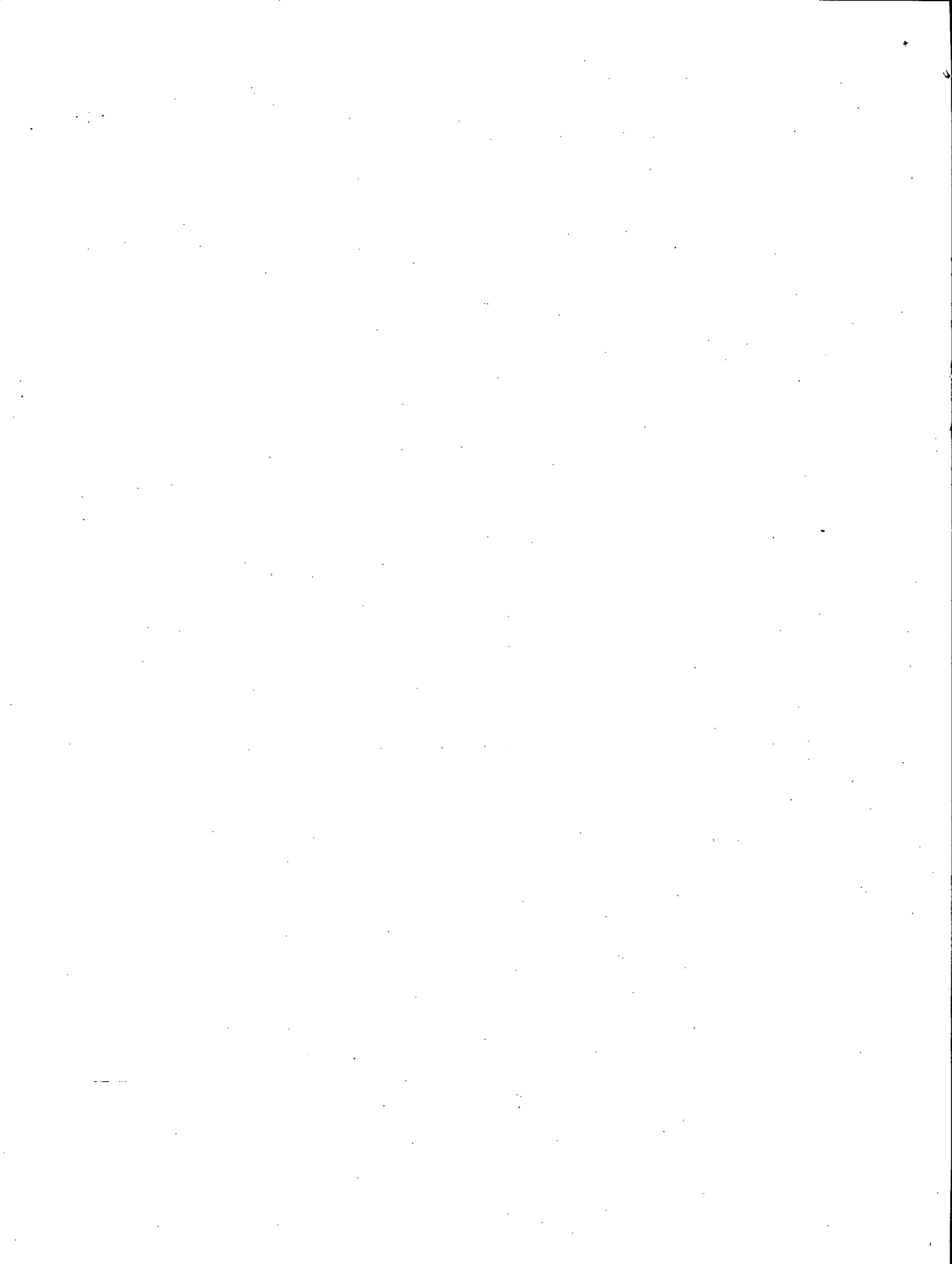
Under the auspices of the Department of Energy, Mines and Resources (EMR), component to the Canadian Nuclear Fuel Waste Management Program (CNFWMP), rock property studies have been carried out and are summarized in this report. After the chapter on the geology of the East Bull Lake Research Area (RA-7), the physical and geophysical rock properties are presented. Chapter 5 contains the assessment of the magnitudes of the various values, attempts comparisons with

other research areas and points out salient features of the data. The main aim of this chapter is to guide those involved in modelling the performance of the rock barrier. The final chapter lists the further work which is i) necessary as the minimum acceptable input for the various models and, ii) useful as additional input for the models.



CHAPTER 2

GEOLOGY



2.1 GENERAL GEOLOGY OF THE EAST BULL LAKE LAYERED COMPLEX

P.J. Chernis

Atomic Energy of Canada Ltd

Whiteshell Nuclear Research Establishment

Pinawa, Manitoba ROE 1L0

P.B. Robertson

Geological Survey of Canada

601 Booth Street

Ottawa, Ontario K1A 0E8

The East Bull Lake complex is an easterly-trending elliptical body located near the southern margin of the Superior Structural Province, 30 km north of Massey, Ontario (Figure 2.1.1). The region is underlain by steeply-dipping Archean metavolcanic and metasedimentary sequences, plus Archean granites and granodiorites emplaced at least 2500 m.a. ago. The East Bull Lake complex is one of three plutonic bodies of possible Proterozoic age which appear to intrude the Archean assemblage. Huronian sedimentary rocks in places unconformably overlie the Archean terrane and possibly the northeastern flank of the East Bull Lake complex as well.

The complex, approximately 13 x 4 km in surface exposure (Figure 2.1.2), comprises a layered series of anorthositic and gabbroic lithologies and the

associated Parisien Lake syenite on its southern flank. The two units are in fault contact, neither intrudes the other, nor do they contain inclusions of the other. Whereas Brown and Kamineni (1980) and McCrank et al (1983) considered the syenite as a separate and unrelated pluton, James et al. (1983) cited similar mafic-felsic associations elsewhere in the region in support of a comagmatic origin. Regardless, since detailed mapping and fracture analyses have been concentrated on, and drilling restricted to the layered basic complex, further compositional and structural data for the syenite are not presented here.

The basic layered complex exhibits fault contacts with both older and younger rocks (marginal dykes) as well as the Parisien Lake syenite. Chilled margins are absent and, with the exception of a possible intrusive relationship with the metavolcanic rocks (McCrank et al., 1983), there are no conclusive indications that the body intrudes the Archean rocks. From these observations, Born and James (1978) suggested that emplacement took place through major tectonic movements, subsequent to crystallization at depth. A pervasive network of diabase dykes, trending WNW, cuts all units of the East Bull Lake body and the surrounding rocks. The Folsom Lake fault parallels this WNW trend, and transects the layered complex dividing it into northern and southern parts.

The basic layered complex comprises a number of arcuate zones which successively mantle a core region situated in the west-central part of the body. Zones are defined from field criteria, such as rock-type and type (or absence) of layering. Some zones consist of metre-scale, cyclical layering of two or more lithologies; others are composed of a single lithologic unit, and particular rock



types may recur in more than one zone. North of the Folsom Lake Fault, the distribution of nine zones was recognized by James et al. (1983) and the attitude of lithologic layering define a shallow, truncated, basin-like structure with inward dips of approximately 20°. The basin configuration is largely not preserved, however, in the part south of the fault. There, a uniformly northeastward shallow dip has been measured and correlation with zones in the northern part is not possible. Brown and Kamineni (1980) suggested that the configuration in the southern portion is due to a zone of small-wavelength folds trending 060°.

All units have undergone metamorphism and/or alteration to the extent that original mineralogy is rarely preserved. However, on the basis of remanent original mineral assemblages, James et al. (1983) defined a succession in the northern part ranging from plagioclase/olivine rocks in the outermost zones, through orthopyroxene- to clinopyroxene-bearing rocks at the core. This lateral succession is consistent with upward progression through a continuously fractionated, basin-like, layered sequence, estimated to be 1 km in thickness. The suite is divided compositionally and physically into a Lower and an Upper Layered Series (James et al., 1983). Olivine norite, troctolitic leuconorite and anorthosite of the Lower Layered Series underlie the northern and eastern regions of the complex. Olivine-free units, norites and gabbros, which define the Upper Layered Series, are largely restricted to a central plateau which is elevated above the Lower Layered Series by a 30 m fault scarp. Detailed mapping of the central plateau by Kamineni et al., (1984) further led to the recognition of

twelve lithologic units, including the basal layered anorthosite of the Lower Layered Series, a number of gabbros distinguished by different textures and types of layering, and a network of granophyre dykes that cuts all other mafic units.

The anorthosites and gabbros consist of calcic plagioclase altered to calcite, epidote and sericite, clinopyroxene replaced to various degrees by calcic amphiboles, red-brown biotite, olivine replaced by tremolite and serpentine or talc, and orthopyroxene replaced by actinolite and Fe-Mg amphiboles. Bright green chlorite replaces both primary and metamorphic minerals adjacent to fractures and veins. Detailed petrography is given in James et al. (1983), Kamineni et al. (1984) and Ejeckam et al. (1985).

The four East Bull Lake research drill holes were collared in the Upper Layered Series in the central plateau. Two holes penetrated granite gneiss at the base of the pluton and established a maximum depth of 770 m (Ejeckam et al., 1985). Subsurface data indicate that lithologic units identified at the surface are correlatable over hundreds of metres. Except for the 450 m-thick basal anorthosite, thicknesses of the layered units are generally less than 120 m. The distribution of dykes is highly variable, ranging from 5-40% by volume in drill holes which are only 600 m apart at the surface.

All units intersected by the holes contain fractures (average fracture density is 15-16/metre). Although the dykes are more highly fractured than other units, the proportion of open fractures is significantly lower. Serpentine, magnetite and chlorite are the principal fracture-filling minerals in troctolite, whereas feldspar, quartz, laumontite and carbonate predominate in the fractures

within anorthosite. A number of rubble zones were encountered containing friable rock, open fractures and numerous microfractures. One such zone is 1 metre thick, occurs at the base of the troctolite unit, and is traceable on a horizontal plane between boreholes. In contrast, a 48 m-thick rubble zone in anorthosite near the bottom of borehole EBL-2 has a near-vertical attitude, and may be correlatable with a prominent surface lineament.

Analysis of surface lineaments from aerial photographs and measurement of fracture orientations and dimensions in outcrop reveal 9 or 10 fundamental strike directions with dips indicative of wrench-faults or regional extension (dip  $-90^\circ$ ), normal faults ( $-60^\circ$ ), thrust faults ( $-30^\circ$ ) and vertical relief extension (subhorizontal). The relative abundance of particular orientations is variable throughout the layered complex. Brown and Kamineni (1980) subdivided the body into a number of kilometre-sized domains of homogeneous fracture characteristics. The central plateau region is characterized by a strong development of steeply-dipping fracture sets at  $040^\circ$ ,  $095^\circ$  and  $175^\circ$  associated with a late-stage deformation, superimposed on less prominent sets at  $170^\circ$ ,  $75^\circ\text{E}$  and  $060^\circ$ ,  $35^\circ\text{N}$ , resulting from an earlier deformation. A detailed interpretation of the deformational history of the East Bull Lake layered complex, which involves up to ten events, has been compiled by Brown and Kamineni (1980) from the distribution of dykes and fractures and the nature of infilling materials.

References

- Born, P. and R.S. James, 1978. Geology of the East Bull Lake layered gabbro anorthosite intrusion, District of Algoma, Ontario. In, Current Research, Part A, Geological Survey of Canada Paper 78-1A, 91-95.
- Brown, A. and D.C. Kamineni, 1980. a reconnaissance survey of structures at the East Bull Lake pluton, Ontario. AECL internal memorandum, 24 pp.
- Ejeckam, R.B., R.I. Sikorsky, D.C. Kamineni and G.F.D. McCrank, 1985. Subsurface geology of the East Bull Lake Research Area (RA-7) in northeastern Ontario. AECL Technical Report TR-348, 35 pp.
- James, R.S., P. Born and J. Bigauskas, 1983. Geology of the East Bull Lake layered complex, District of Algoma, Ontario. In, Current Research, Part B, Geological Survey of Canada paper 83-1B, 1-11.
- Kamineni, D.C., G.F. McCrank, D. Stone, R.B. Ejeckam, R. Hindall and A. Sikorsky, 1984. Geology of the central plateau of the East Bull Lake pluton, northeastern Ontario. In, Current Research, Part B, Geological Survey of Canada Paper 84-1B, 75-83.
- McCrank, G.F.D., D. Stone, D.C. Kamineni, B. Zayachkivsky and G. Vincent, 1983. Regional geology of the East Bull Lake area, Ontario. In, Current Research Part A, Geological Survey of Canada Paper 83-1A 457-464.

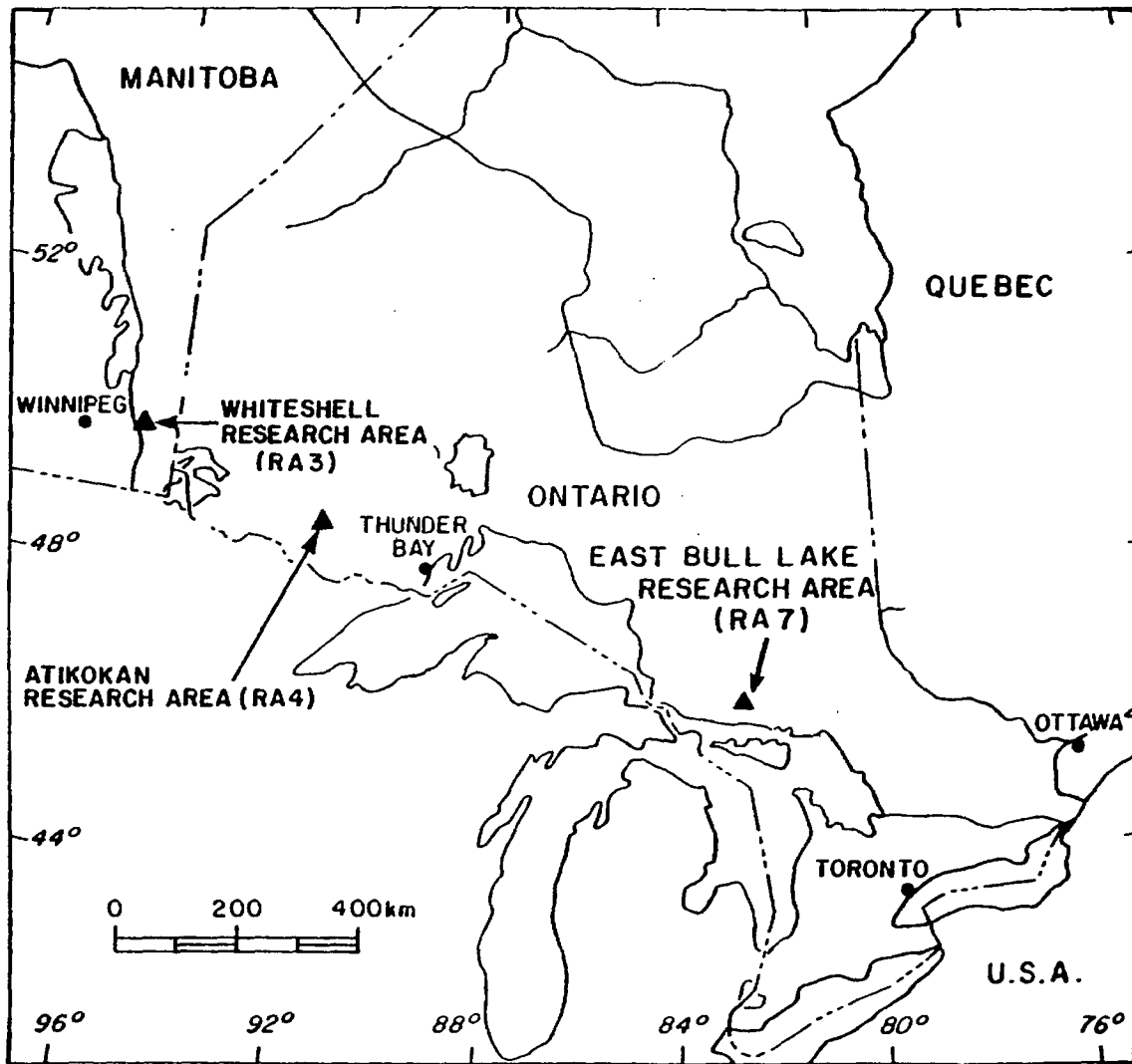


Figure 2.1.1 Location of East Bull Lake Research Area.



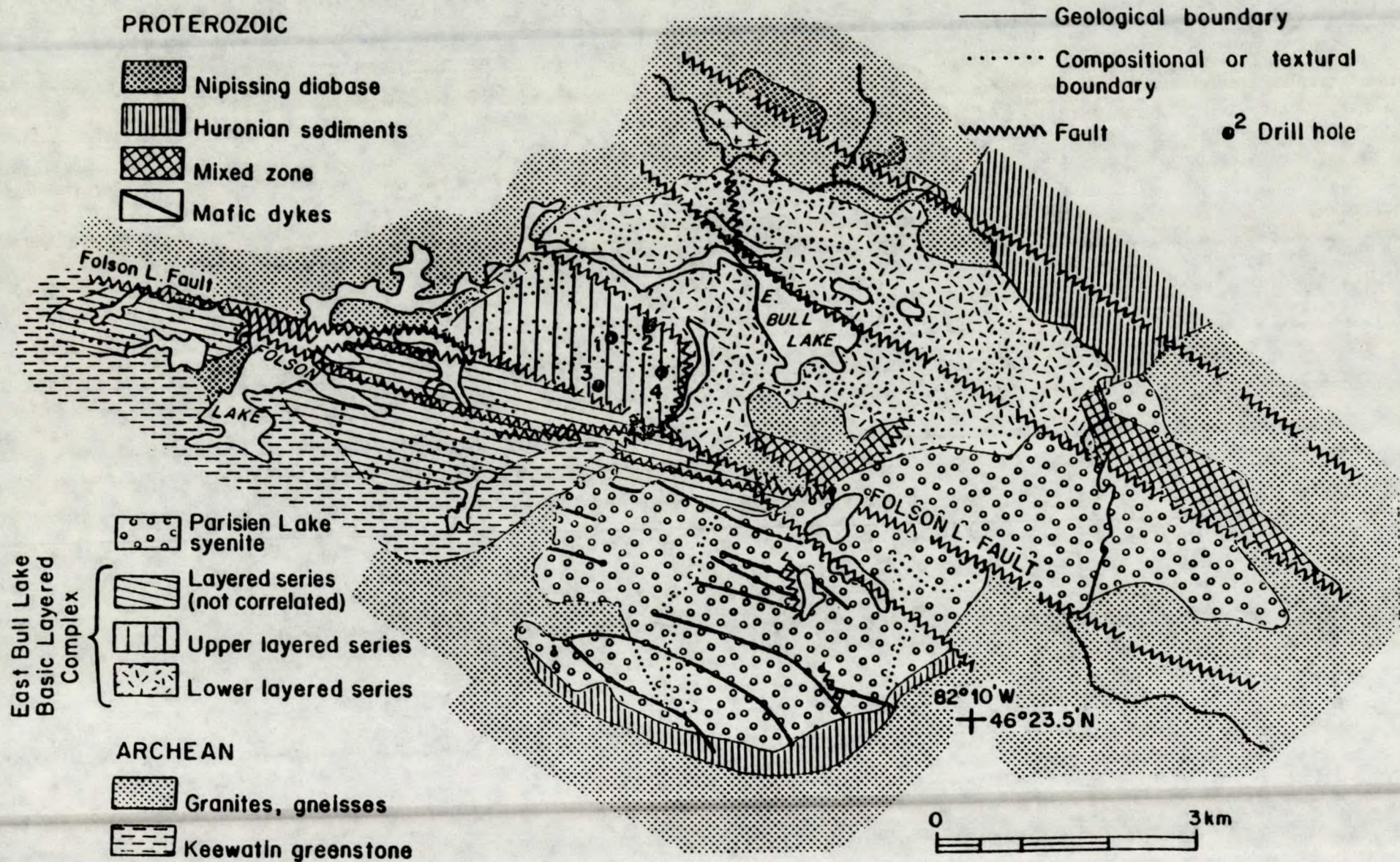


Figure 2.1.2 General Geology of the East Bull Lake Research Area.



## 2.2 PORE- MICROCRACK STRUCTURES

P. J. Chernis

Atomic Energy of Canada Limited

Whiteshell Nuclear Research Establishment

Pinawa, Manitoba

ROE 1 LO

### 2.2.1 Introduction

Microcracks and micropores are defined as those cracks that have at least one dimension that can be resolved only with magnification ( $< 0.2\text{mm}$  wide), whereas dimensions of macrofractures and veins can be measured with the unaided eye. Microcracks influence mechanical and hydrogeologic properties of rocks. Therefore, their occurrence, formation, and evolution were studied as part of the concept assessment phase of the Nuclear Fuel Waste Management Program. Microcrack structures in quartz-poor, gabbroic-anorthosites from the East Bull Lake layered complex, Ontario, and in low porosity, quartz-bearing granitic rocks from the Lac du Bonnet Batholith, Manitoba, and the Eye-Dashwa Lakes Pluton, Ontario, have been examined. It has been demonstrated that quartz is an important site for microcracks in the granitic rocks (Chernis, 1984a, 1984b, 1985). Microcracks in these rocks formed as the rocks contracted upon cooling, and as a brittle response to stress. In contrast, unfractured, quartz-poor

mafic dikes are known to have very low porosity (Brace, 1965), but the porosity of gabbroic-anorthosite samples, examined here, varies widely. In the gabbroic-anorthosites, cooling microcracks are healed, and many cracks formed by tectonic stress have been filled by secondary minerals.

### 2.2.2 Microcracks in gabbroic-anorthosite

The porosity of samples varies by more than an order of magnitude from less than 0.5% to more than 5%. Relatively unfractured, lowest-porosity samples of the gabbroic-anorthosite contain few micropores and microcracks: pre-existing microcracks which formed as the rocks cooled are sealed with chlorite or other secondary minerals. Intragranular cracks in plagioclase are filled by chlorite (Plate 1). Narrow chlorite veins and calcite veins (<1 mm wide) possess microscopic and macroscopic open segments along their edges and in their centres. Fractured samples contain healed, prehnite-bearing macrofractures (veins) up to 5 mm wide. Open spaces in these veins are parallel to the vein walls. They vary from rough-walled microcracks less than 2  $\mu\text{m}$  wide (Plate 2), which appear to the naked eye as white traces along portions of the centres and edges of the veins, to 0.5 mm wide by cm-long macrofractures which formed after the veins crystallized. Latest fractures have only small amounts of mineral infillings (Plate 3). Intensified microcrack healing in the rock matrix adjacent to prehnite veins, when compared to matrix removed from prehnite veins, is reflected by lowered geometric mean crack width (0.32 $\mu\text{m}$  vs 0.46 $\mu\text{m}$ ), crack porosity (0.083% vs 0.187%), and crack density (0.24/mm vs 0.66/mm). Microcracks



everywhere in the matrix have rough walls (Plate 4). Micropores which are remnants of pre-existing cracks are locally abundant both in the rock matrix (Plate 5) and in the prehnite veins (Plate 6). The abundance of micropores in plagioclase grains ranges from less than 1% porosity (<10 pores of <1  $\mu\text{m}$  in size per 100  $\mu\text{m}^2$ , to porosities of 10-15% and pore sizes of <1 $\mu\text{m}$  to 100  $\mu\text{m}$ . Pores and microcracks also occur within and around microscopic quartz blebs (<50  $\mu\text{m}$  in size, average approximately 10  $\mu\text{m}$ ) which are byproducts of the alteration of primary plagioclase. Pores in prehnite veins are generally less than 10 $\mu\text{m}$  in size, and locally comprise up to 10% of the veins by volume. The porosity of secondary amphiboles is highly variable, and can be as high as 3.8%. It is due to cleavage cracks, these having an average width 0.71 $\mu\text{m}$  (standard deviation 0.58  $\mu\text{m}$ , geometric mean 0.48 $\mu\text{m}$ ) (Plate 7).

### 2.2.3 Concluding remarks

To summarize, quartz, although an important site for microcracks in granitic rocks, is not a primary mineral, nor is it an abundant secondary mineral in gabbroic-anorthosites of the East Bull Lake layered complex. Cooling cracks in plagioclase have been sealed by secondary chlorite, albite, and epidote. For these reasons, before they were tectonically stressed and fractured, the gabbroic-anorthosites contained few microcracks and micropores and had very low porosities. The porosity of the rocks from the East Bull Lake layered complex is now highly variable on a centimetre scale, and is a result of the extent to which penetrative fractures developed during an early phase of brittle deformation, on

subsequent pore and crack filling/sealing by secondary minerals, and on formation of new fractures and the reactivation of old, sealed fractures (veins). Fracturing and fracture-sealing have resulted in bulk porosities of <0.5 to >5% and locally as high as 15%. Much of the significant existing fracture porosity is attributed to the latest fracturing event which was not accompanied by deposition of large amounts of low-temperature secondary minerals. Compared with granitic rocks from the Eye-Dashwa Lakes Pluton and the Lac du Bonnet Batholith, fractured gabbroic-anorthosites from the East Bull Lake complex have considerably larger mean crack widths, a consequence of intense penetrative brittle deformation, but extremely small crack densities, the results of extensive crack healing.

REFERENCES

- Brace, W.F., 1965. Some new measurements of linear compressibility of rocks. *Journal of Geophysical Research*, V.70, p.391-398.
- Chernis, P.J. 1983. Notes on the pore-microfracture structure of some granitic samples from the Whiteshell Nuclear Research Establishment. Atomic Energy of Canada Limited Technical Record TR-226. 34p.
- Chernis, P.J. 1984a. Comparison of the pore-microcrack structure of shallow and deep samples of the Lac du Bonnet granite. Atomic Energy of Canada Limited Technical Record TR-223. 20p.
- Chernis, P.J. 1984b. The effects of crack healing on the microcrack structure of core samples from borehole ATK-1, in the Eye-Dashwa Lakes Pluton, Northwestern Ontario. Atomic Energy of Canada Limited Technical Record TR-268.
- Chernis, P.J. 1985. Microcrack structures in plutonic rocks from the Whiteshell Nuclear Research Establishment, Eastern Manitoba, and Atikokan, Northwestern Ontario. Unpublished M.Sc. Thesis, Carleton University, Ottawa. 159p.
- Chernis, P.J. 1986. Scanning electron microscopy of pore-microcrack structures in gabbroic-anorthosites from the East Bull Lake layered complex, near Massey, Ontario. To be submitted as an AECL TR-Series Report (in preparation).

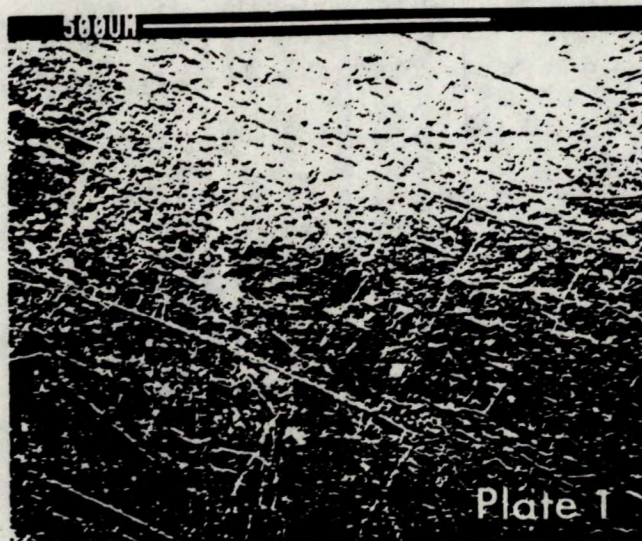


Plate 1. Pre-existing Cracks in Plagioclase Healed by Chlorite.

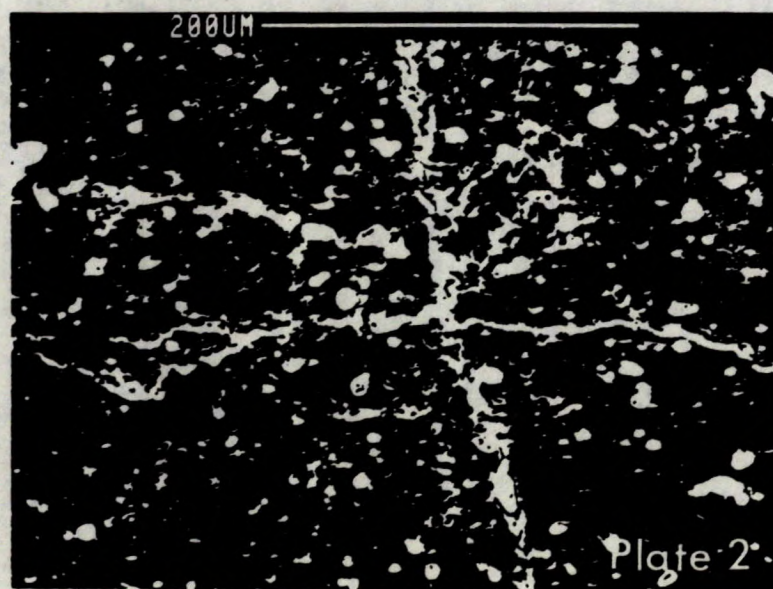


Plate 2. Micropores and Narrow Rough-Walled Microcracks in the Centre of a 10 mm Wide Prehnite Vein.

Plate 3. Microcrack Traversing Plagioclase and Mafic Grains: Contains a Small Amount of Mineral Infilling. Light coloured filling is a sheet silicate. This fracture has the form of fresh, sharp-tipped, en-echelon, drill-related, stress-induced cracks observed in the Lac du Bonnet Granite (Chernis, 1984a, c). Note the paucity of pores in the plagioclase through which this crack passes.



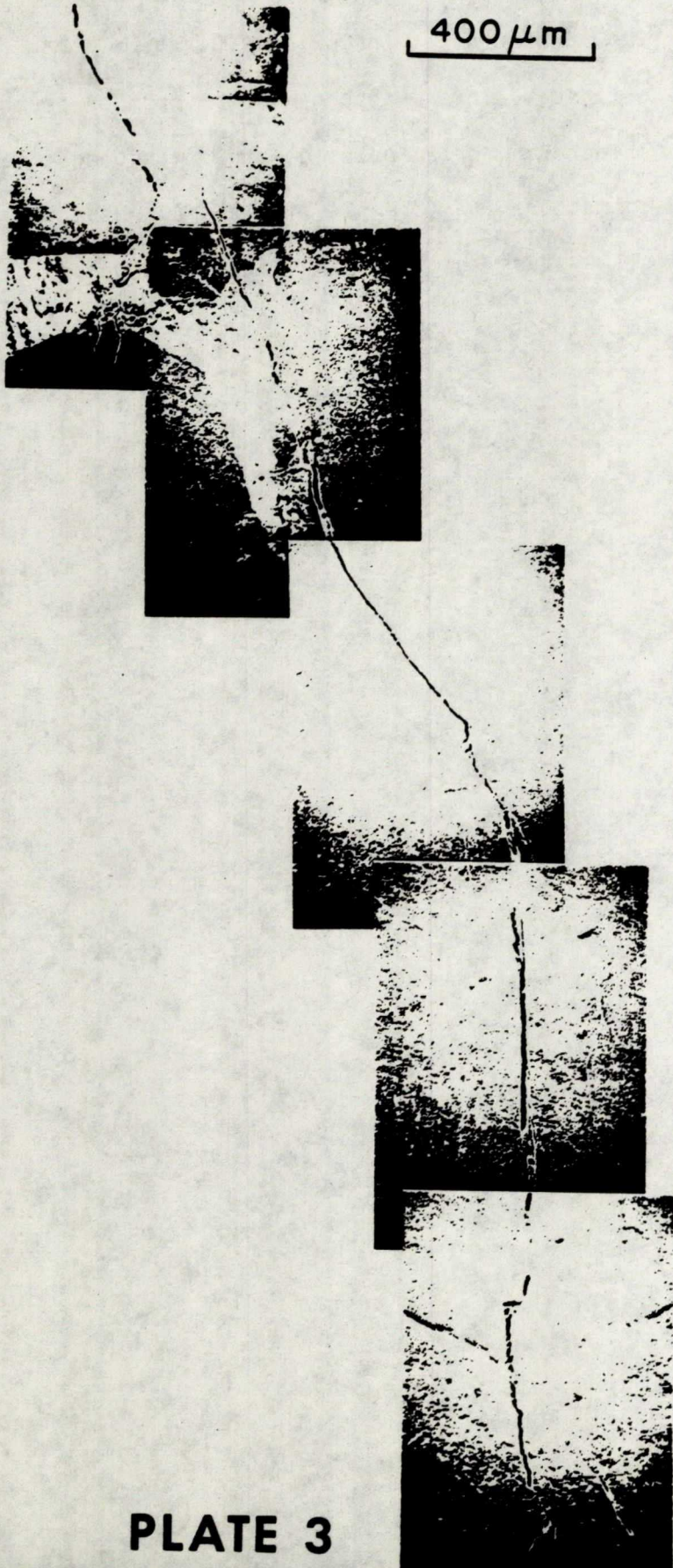


Plate 4. Pre-existing Cracks Vary from Rows of Elongate Pores to  
Densely-Bridged, Rough-walled Cracks.



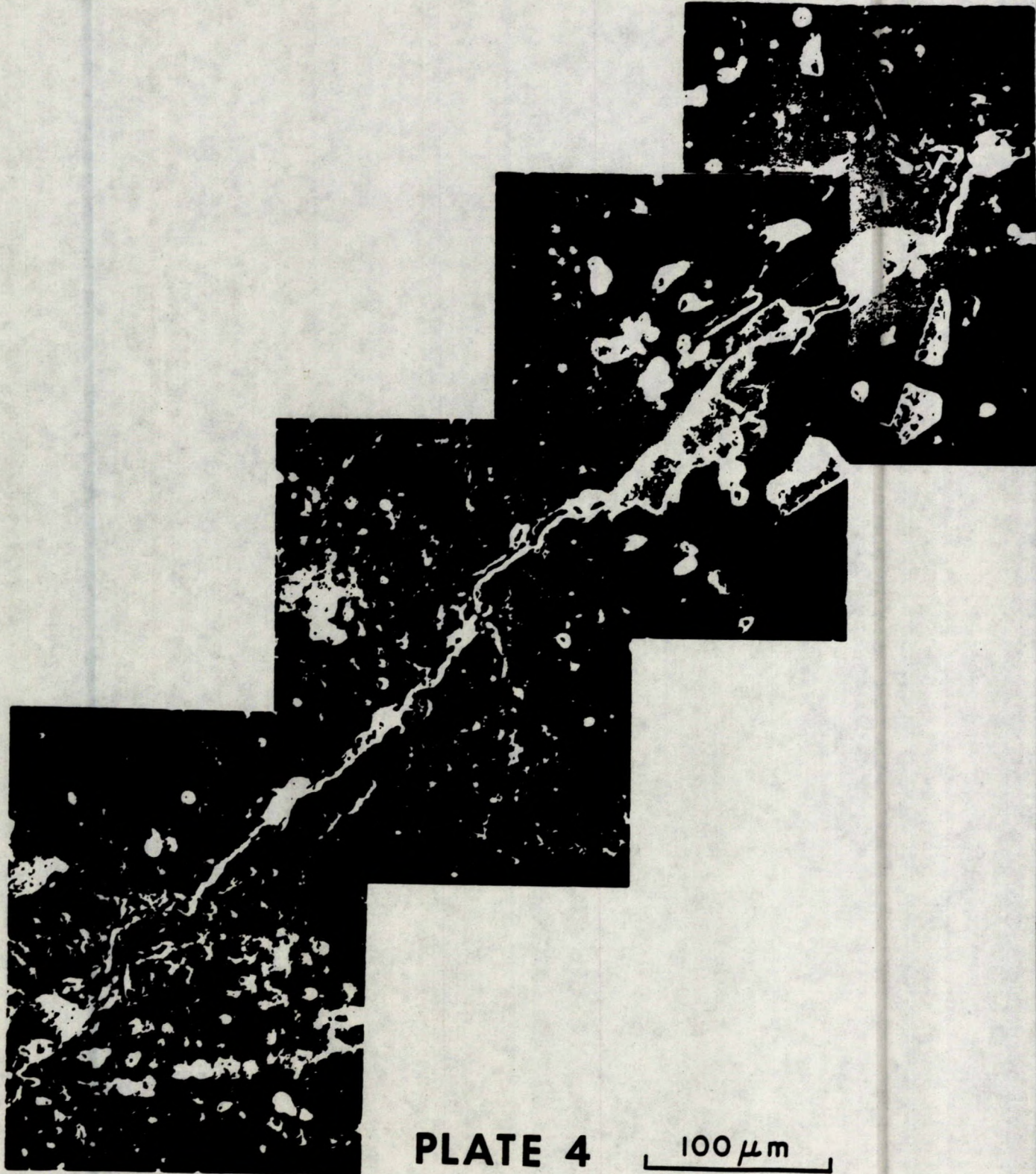


PLATE 4

100 μm



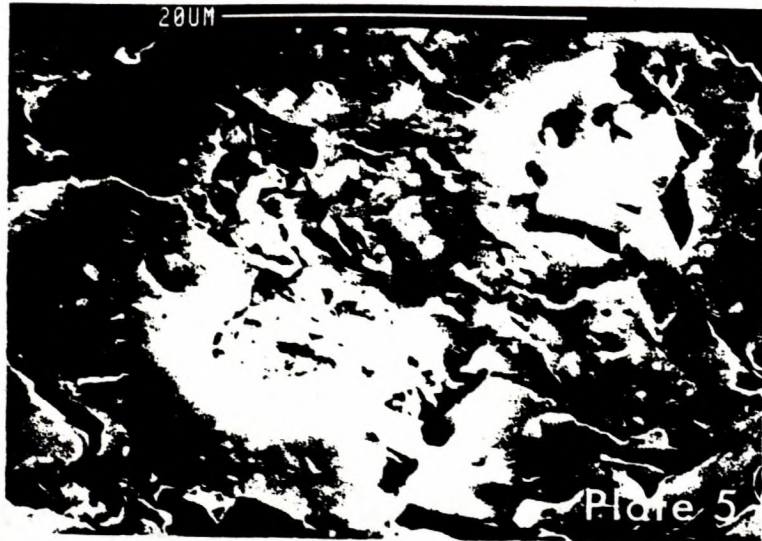


Plate 5. High Densities of Micropores in Matrix Plagioclase.



Plate 6. A 10 mm Wide Prehnite Vein Containing High Densities of Micropores.



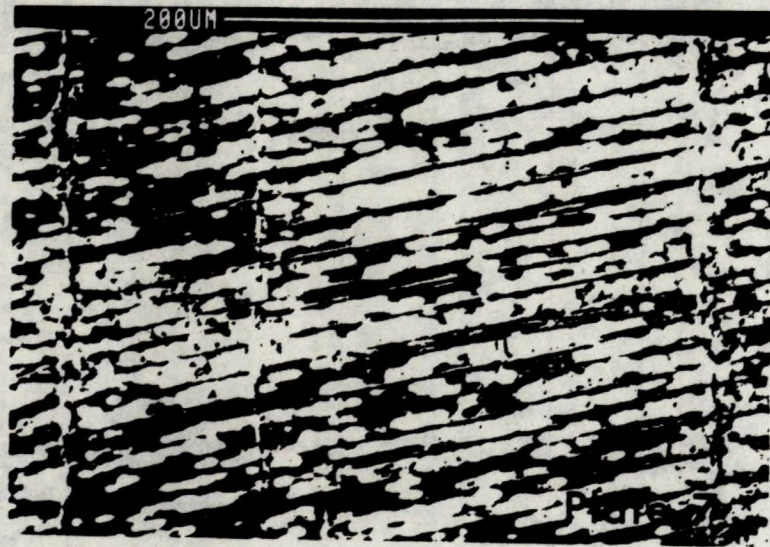
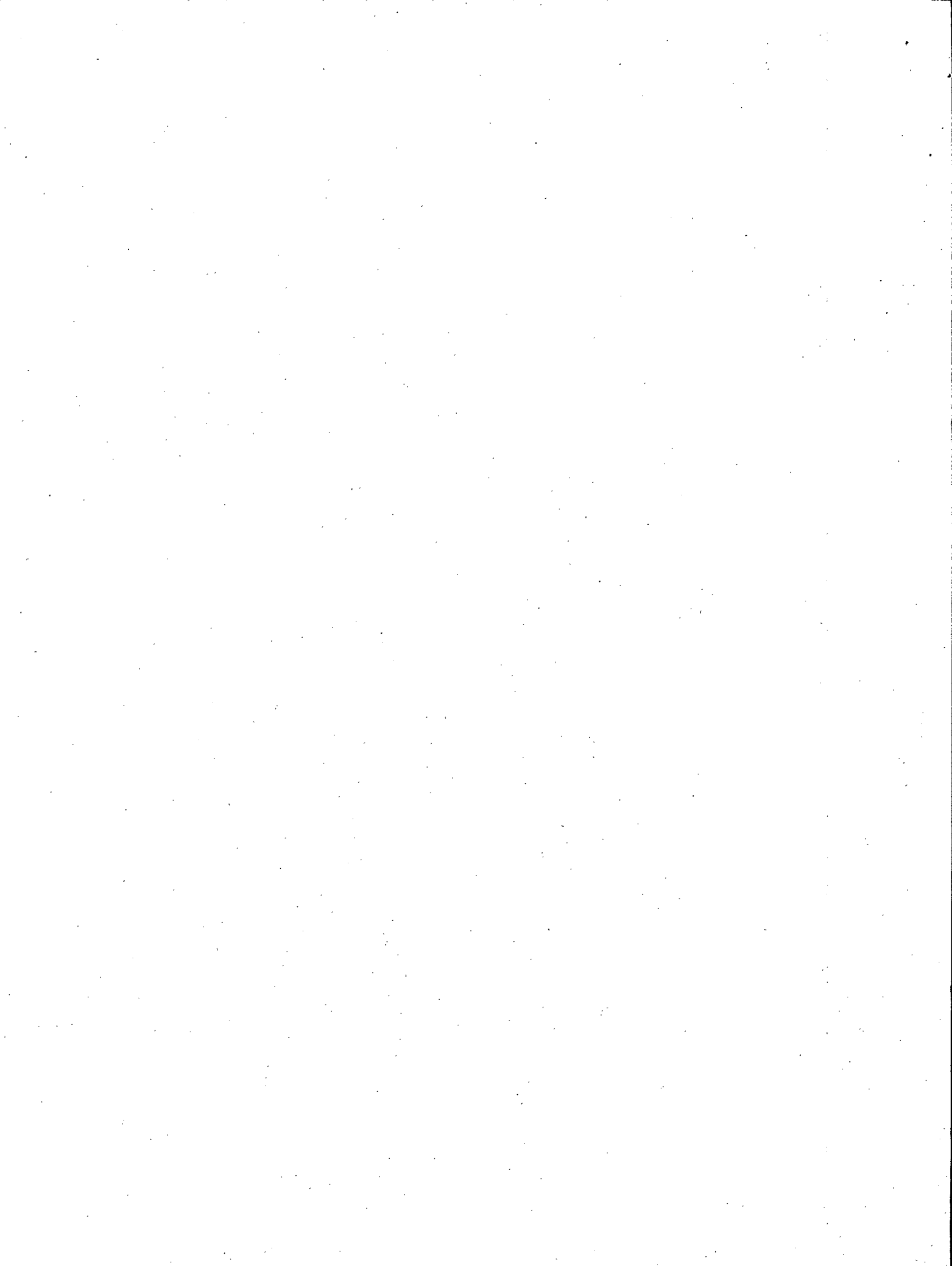


Plate 7. Mica and Amphibole Grains May Contain Large Numbers of Cleavage Cracks.

CHAPTER 3

PHYSICAL PROPERTIES



3.1 MECHANICAL PROPERTIES

A. Annor

Canada Centre for Mineral and Energy Technology (CANMET)

555 Booth St.,

Ottawa, Ontario

K1A 0G1

R. Jackson

Atomic Energy of Canada Ltd.

Whiteshell Nuclear Research Establishment

Pinawa, Manitoba,

ROE 1LO

3.1.1 Introduction

A principal objective of the Canadian Nuclear Fuel Waste Management Program (NFWMP) is the safe management of nuclear fuel wastes so that there will be no major adverse effects on man or environment at any time (Simmons, 1984). Towards this end, the suitability of long term emplacement in deep geological formation is being studied.

A vital step in the design, construction and monitoring of such a facility involves the determination of the mechanical properties of the host rock. For purposes of engineering analysis two models are generally required for evaluating

rock mass stability. These are:

- (a) the strength and deformation model of the intact rock material,  
and
- (b) the strength and deformation model of the joint systems present in  
the rockmass.

The predictive models must be developed to include ambient stress and temperature conditions that exist in the rockmass, as well as changes that could be expected due to thermal loading. The variation of the strength and deformational properties with depth is also required in order to identify zones of weakness in the rock mass.

Over the past few years, CANMET, in conjunction with Atomic Energy of Canada Limited (AECL), has carried out mechanical and thermomechanical rock property investigations in support of the NFWMP research efforts. The objectives of these studies have been:

- to develop and assess equipment and methodologies for characterizing rock samples,
- to develop and test physical property models, under ambient conditions of temperature and pressure, and
- to acquire mechanical rock property data for samples from the East Bull Lake pluton and to evaluate it for modelling studies.

### 3.1.2 Tests

Uniaxial compression strength tests were carried out in order to obtain the

unconfined strength and deformational parameters of the rock samples. Bulk density of the test samples were determined to permit comparison of the established mechanical properties with data in the published literature.

Compressive wave velocity measurements were carried out in order to identify possible interrelationships between static and dynamic elastic properties with stress, and to help in the eventual development of seismic monitoring techniques.

### 3.1.3 Rock samples

Nineteen gabbroic rock samples were tested. The samples originated from various levels in boreholes and they were considered to be representative of the borehole lithology. Geological description of the East Bull Lake pluton and the test samples are provided by Ejeckam et al., (1985) and in CHAPTER 2.

### 3.1.4 Experimental methods

Sample preparation, equipment and testing procedures conformed closely with the following standards and specifications: CANMET Pit Slope Manual Specifications (Gyenge and Herget, 1977), American Society for Testing and Materials (ASTM 1971, 1979); and the International Society for Rock Mechanics (ISRM), Suggested Methods (Brown, 1981). The testing procedures are also described elsewhere (Jackson and Paquette, 1984).



### 3.1.5 Discussion and conclusions

The mechanical properties established for the individual samples were summarized by Jackson and Paquette (1984). A statistical summary of the test results is provided in Table 3.1.1 and a summary of test data in Table 3.1.2. The values are within the range of values in the published literature for the type of gabbro found in the East Bull Lake pluton (Lama and Vutukuri, 1978; Touloukian and Ho, 1980). Additional test data from uniaxial compressive and tensile strength tests as well as triaxial compression measurements, at ambient and elevated temperatures, are required in order to develop the necessary strength and deformational models for characterizing the rock mass and to meet concept assessment requirements more rigorously.



REFERENCES

- ASTM, 1971a. Standard test for unconfined compressive strength of intact rock specimens; ASTM Test D2927-71(a).
- ASTM, 1971b. Standard test for splitting tensile strength of cylindrical concrete specimens; ASTM Test C496-71.
- Brown, E.T. (Ed.) "Rock characterization, testing and monitoring, ISRM suggested methods"; Pergamon Press 107-127.
- Ejeckam, R.B., Sikorsky, R.I., Kamineni, D.C. and McCrank, G.F.D. "Sub-surface geology of the East Bull Lake research area (RA7), in Northeastern Ontario"; AECL Technical Record RT-348, Pinawa, Manitoba.
- Gyenge, M. and Herget, G. "Pit Slope Manual Supplement 3-2; Laboratory tests for design parameters"; CANMET Report 77-26; CANMET, Energy, Mines and Resources Canada; Ottawa; 1977.
- Jackson, R.D. and Paquette, D. "Compressional wave velocity, Young's modulus, Poisson's ratio and uniaxial compressive strength for EBL 2 and EBL 4 samples from East Bull Lake"; Division Report MRP/MRL 84-86 (INT); CANMET, Energy, Mines and Resources Canada, Ottawa, 1985.
- Larocque, G.E. and Annor, A. "Overview: rock mechanics/rock properties"; 17th Nuclear Fuel Waste Management Information Meeting Proceedings; Ottawa, February 1984; Atomic Energy of Canada Ltd. Technical Record TR-299, Pinawa, Manitoba (in preparation).

Lama, R.D. and Vutukuri, V.S. "Handbook on mechanical properties of rocks II";

Trans Tech Publications; Clausthal, Germany; 1978.

Touloukian, Y.S. and Ho, C.Y. "Physical properties of rocks and minerals";

McGraw-Hill/CINDAS Data Series on Material Properties; McGraw-Hill Book Company II-2:29-176; 1981.

Simmons, G.R., Annor, A., Baumgartner, P., Lang, P.W., Larocque, G.E. and

Wilkins, B.J. "The geomechanics program - A review"; Proceedings of the

18th Information Meeting on the Nuclear Waste Management Program (1984

General Meeting); Atomic Energy of Canada Limited, Whiteshell Nuclear

Research Establishment, Pinawa, Manitoba; Report No. (TR-320); 23-44 pp;

1984.

Table 3.1.1 Statistical summary of unconfined mechanical properties for rock samples from East Bull Lake pluton

Borehole identif- cation	Principal rock type	No. of samples tested		Bulk density (Mg/m <sup>3</sup> )	Uniaxial compressive strength (MPa)	Young's modulus (GPa)	Poissons' ratio	P-wave velocity at zero press. (km/s)
EBL 2	Gabbro	8	No. of values	8	8	8	8	8
			Range	2.82-2.90	160-233	58.57-88.46	0.20-0.31	5.04-7.14
			Mean	2.86	184	77.43	0.27	6.38
			Std. Dev.	0.03	33	11.53	0.04	0.81
EBL 4	Gabbro	11	No. of values	11	11	11	11	11
			Range	2.87-3.11	110-316	78.39-116.87	0.23-0.33	6.80-7.20
			Mean	2.94	215	95.49	0.28	7.05
			Std. Dev.	0.08	60	10.81	0.03	0.12
EBL 2 & EBL 4 (combined)	Gabbro	19	No. of values	19	19	19	19	19
			Range	2.82-3.11	110-316	58.57-116.87	0.20-0.33	5.04-7.05
			Mean	2.91	202	86.91	0.27	6.77
			Std. Dev.	0.08	50	14.87	0.03	0.62

Table 3.1.2 Summary of uniaxial mechanical properties and compressional wave test data for East Bull Lake rock samples

Sample identification	Young's modulus (GPa)	Poisson's ratio	Uniaxial compressive strength (MPa)	Zero pressure compressive wave velocity (km/s)	
EBL 2	419.92	75.20	0.31	165	6.99
	449.18	85.04	0.31	196	7.14
	548.20	72.70	0.23	188	6.67
	613.50	88.06	0.23	149	7.10
	692.75	68.44	0.26	168	5.96
	734.10	58.57	0.26	213	5.04
	767.20	64.35	0.50	160	5.40
	804.00	88.46	0.28	233	6.77
EBL 4	25.00	78.39	0.28	144	7.08
	37.00	106.22	0.28	316	6.98
	57.60	96.55	0.23	267	6.80
	87.50	96.57	0.26	244	6.98
	123.10	116.87	0.31	228	7.13
	150.32	104.74	0.27	262	7.01
	206.70	89.65	0.28	172	7.20
	250.70	91.80	0.27	179	7.08
	298.30	91.03	0.33	222	7.11
	325.10	95.31	0.28	223	7.24
	375.80	83.27	0.32	110	6.97

3.2

PORE STRUCTURE CHARACTERISTICS

J.P. Hume

Atomic Energy of Canada Limited/

Geological Survey of Canada

601 Booth Street, Ottawa, Ontario

K1A 0E8

and

T.J. Katsube

Geological Survey of Canada

601 Booth Street, Ottawa, Ontario

K1A 0E8

3.2.1 Introduction

The concept of using a deep rock vault for nuclear waste necessitates the development of the technology to predict accurately the rate of radionuclide migration through the host rock assuming that radionuclide release from the vault is possible. A pluton contains a network of fractures with apertures that range from a few hundredths of micrometers to a few hundred micrometres (Katsube and

Hume, 1986 and section 2.2). The dominant mechanism for radionuclide migration in the smaller fractures is diffusion. Advection predominates in larger fractures. Diffusion will also retard the flow of radionuclides along fractures. The equations that govern diffusion in plutonic rocks (Wadden and Katsube, 1982; Katsube and Hume, 1986) are:

$$J = \frac{D}{F} \frac{\partial C}{\partial X}$$

$$\frac{\partial C}{\partial t} = \frac{D^2}{\tau} \frac{\partial^2 C}{\partial t^2}$$

where,

J = diffusion flux,

D = diffusion coefficient of the diffusing species,

C = concentration of diffusing species,

x = distance in the direction of diffusion,

t = time,

$\tau$  = tortuosity,

F = formation factor.

Advection is considered insignificant in unfractured mafic rocks (Katsube and Hume, 1986).

As indicated by these equations, formation factor (F) and tortuosity ( $\tau$ ) are the two pore structure parameters that most strongly control radionuclide

migration through these rocks. This paper reports the results of the study on the pore-structure parameters of mafic rock samples from East Bull Lake research area.

The formation factor is the ratio of the tortuosity over the connecting porosity, and is also defined as the ratio of the resistivity of a rock saturated with an electrolyte to the resistivity of the electrolyte (Archie, 1942). The connecting porosity ( $\phi_C$ ) is a parameter related to the pore space in the connecting pores through which the migrating species diffuse or flow. See Katsube and Kamineni (1983) or Katsube and Hume (1986) for the precise definition of this parameter. The tortuosity ( $\tau$ ) is the ratio of the actual length along the pore path between two points in a rock over the spatial distance between these two points (Katsube and Kamineni, 1983). The formation factor can be measured directly, but tortuosity must be derived from the actual measurements of effective porosity ( $\phi_E$ ) and formation factor (F). The methods for measuring these parameters are described in Katsube (1981), for example. Based on the model described in Katsube and Kamineni (1983) or Katsube et al (1985), connecting porosity ( $\phi_C$ ) and tortuosity can be derived from effective porosity ( $\phi_E$ ) and formation factor (F) by using the following equations:

$$\phi_C = \phi_E / F \quad (1)$$

$$\tau = \phi_E / F \quad (2)$$

In this case, it is assumed that the pocket porosity ( $\phi_p$ ) is equal to zero. Pocket porosity ( $\phi_p$ ) is the porosity of the blind and pocket pores which do not contribute to the migration of radionuclides. In fact, these pores may retard the migration.

Pore structure data reported in the literature for mafic plutonic rocks is almost non-existent. The effective porosity ( $\phi_E$ ) for gabbro reported by Alexander et al (1981) is in the range of 0.30-0.52%. The data reported by Katsube et al (1985) for the rock samples from Chalk River research area, which includes gabbros and diabases as well as all kinds of gneisses, is in the range of 0.1-0.84%. The formation factor and tortuosity values obtained by Katsube et al (1985) for the same rocks are in the range of 990- $5.3 \times 10^5$  and 8.0-40., respectively. Porosity, formation factor and tortuosity for granites lie within the ranges of 0.1-0.6%,  $10^3$ - $10^6$ , and 2.4-3.7, respectively, (Katsube and Hume, 1986).

### 3.2.2 Samples

A total of 33 standard, unfractured samples were selected from boreholes EBL-2 and EBL-4. The lengths of boreholes EBL-2 and EBL-4 are approximately 835 m and 489 m, respectively, and the diameter of the core was about 4.5 cm. Samples were chosen from four of the five lithological units identified by Kamineni et al (1984): (troctolite, massive gabbro and dendritic and anorthositic gabbro).

A suite of 14 unoriented large hand specimens (up to  $0.5\text{m}^3$ ) representing a



variety of rock types was also collected from the surface outcrops in the East Bull Lake research area (Percival et al in prep.). Four representative rock types (mafic dykes, gabbros, syenite and granodiorite) were sampled in the central plateau area of the pluton. Two samples (#1 and 14) were taken from a mafic dyke commonly referred to in the field as the "black" dyke. One sample (#3) was taken from a mafic dyke referred to as the "green" dyke. Proximal to the black dyke were dendritic gabbro and massive gabbro units. One sample (#13) was taken from the dendritic unit and another (#2) from the massive gabbro unit. From east & northeast of Bull Lake, four massive gabbro samples (#6, 7, 11 and 12) and one anorthositic gabbro sample (#8) were collected from the rhythmic layered gabbro and anorthosite map units. Two Nipissing Diabase samples (#9 and 10) were collected from an area about 3 km east of East Bull Lake. Samples #4 and #5, a granodiorite and coarse-grained syenite, respectively, were collected from a rock dump to complete the spectrum of characteristic rock types.

### 3.2.3 Experimental Methods

The surface hand samples were cored at Canada Centre for Mineral and Energy Technology (CANMET) facilities using a 4.5-cm bit (Long Year Christensen) with an Ibarria (model 30-CA) drill press. Samples were oriented in such a way as to obtain core of 2 cm to 25 cm in length in 2 or 3 mutually perpendicular directions (labelled A, B and C). The core was then cut, using a diamond saw, into a series of discs of variable length (1 cm to 5 cm). Several small discs (1 cm) from each core were used for immersion porosity and formation resistivity

factor measurements. Uncut portions of the core were used to make thin sections and provide crushed material for geochemical analyses.

The effective porosity ( $\phi_E$ ) and formation factor (F) were determined, but permeability measurements are not yet available. The effective porosity ( $\phi_E$ ) of EBL surface and subsurface samples was obtained using an immersion technique (Katsube and Hume, 1986), which involves determining the pore volume of a sample from the difference between its water saturated and oven-dry weight. The bulk volume of a rock sample is calculated from its length and diameter.

The formation factor (F), the ratio of the resistivity of a rock completely saturated with an electrolyte to the resistivity of the electrolyte, was measured using the system described by Gauvreau and Katsube (1975). The rocks are vacuum-saturated in distilled water for 15 minutes and then allowed to stand (still immersed in distilled water) for 24 hours prior to performing resistivity measurements. The apparent formation factor is determined by repeating this procedure using a series of five saline solutions ranging in concentration from 0.02 to 0.50 M. The procedure described by Katsube (1981) and Worthington (1975) is then used to calculate the apparent formation factor of a sample.

#### 3.2.4 Results

The minimum, maximum, mean and standard deviation for measured pore structure parameters are summarized in Tables 3.2.1 and 3.2.2. Measured pore structure parameters for individual samples including formation factors, effective porosity and tortuosity) from the paper by Percival et al., (in prep.) are

compiled in Tables 3.2.3 and 3.2.4. A significant degree of anisotropy was found in some samples (Percival et al in prep.). The anisotropy coefficient ( $\lambda$ ) is defined as follows (Percival et al in prep.):

$$\lambda = \frac{x}{x_1} \quad (3)$$

where  $x$  = property of a sample measured in any given direction

$x_1$  = property measured in a direction perpendicular to  $x$

In this case  $x$  and  $x_1$  are sample formation factors.  $F$  values were selected in such a way that  $\lambda$  is always greater than 1.0. Coefficient of anisotropy data ( $\lambda$ ) is compiled in Table 3.2.5, and summarized in Table 3.2.2.

Formation factor values in the samples ( $F$ ) range from about  $10^3$  to  $10^6$  for both surface and subsurface samples. Similar values have been reported in the literature and measured with respect to granite samples (Katsube and Hume, in prep.). However, the values of the surface samples are skewed towards the lower limit with a mean of  $5 \times 10^3$ , and the subsurface samples are skewed towards the upper limit with a mean of about  $10^5$ . The formation factor values of the surface samples are generally in the range of  $10^3$ - $4 \times 10^4$  with values above  $4 \times 10^4$  representing mainly mafic dykes. The formation factor values of the subsurface samples are generally in the range of  $2.5 \times 10^4$  to  $10^5$ ; values below  $2.5 \times 10^4$  correspond mainly to troctolites. Samples equivalent to troctolites are not included in the surface suite of samples, and samples equivalent to mafic dykes are not included in the subsurface suite of samples. Therefore, in general, the

formation factors for the subsurface samples are more than an order of magnitude larger than those of the surface samples.

The values of effective porosity ( $\phi_E$ ) are in the range of 0.04 to 1.0% for the surface samples, and 0.025 - .63% for the subsurface samples. These ranges are slightly wider than those reported in the literature, and for the Chalk River samples (see the introduction to this paper). However, the effective porosities ( $\phi_E$ ) of the surface samples are skewed towards the upper limit with a mean value of 0.23%, and values of subsurface samples are skewed towards the lower limit with a mean value of 0.09%. The values of the mafic dyke samples (surface samples) are under 0.16%.

The tortuosity range is 1.0 to 25 for the surface samples, and 1.0 to 40 for the subsurface samples. The mean value for the surface samples is 3.7, and 9.9 for subsurface samples. It is mainly the troctolites which have the lower values. These ranges are, in general, similar to those reported by Katsube et al., (1985). However, the lower limit of the EBL samples is considerably below the limit for some gabbros.

The values for the coefficient of anisotropy reported by Percival et al (in prep.) for the surface samples range between 1.0 to 50, but are generally in the range of 1-6.3, with values above the upper limit being considered anomalous. The anomalous values belong to 5 samples of which 3 are mafic dykes. The other two values belong to a massive gabbro and a dendritic gabbro sample. Since 3 out of 5 of the mafic dyke samples show anomalously high values of tortuosity compared to 2 out of 7 of the gabbros, mafic dykes may be considered more

anisotropic than the other rock types.

### 3.2.5 Discussion and conclusions

The values of formation factor, effective porosity and tortuosity of the EBL samples are generally within the ranges reported in the literature for similar rock types, although some of the values are higher for  $F$  and  $\tau$ , and lower for  $\phi_E$ , when compared specifically with those of granites. Little data is available in the literature for the anisotropy coefficient. Within the EBL surface samples, most of those from dykes show anomalously high values for  $F$ , and low values for  $\phi_E$ . About 60% of the dyke samples, and about 30% of the metagabbro samples show anomalously high values of  $\lambda$ . Within the subsurface samples, the troctolites tend to show lower values of  $F$ . There are no equivalent samples included in the surface samples.

There are a number of methods which, in using the interrelationship between the different parameters, allow characterization of the rocks (Katsube and Hume, in prep.). Data for the "Archie method" and "pocket porosity method" are available in this study. The well known Archie relationship is expressed by the following equation:

$$F = \frac{a}{\phi_E^m} \quad (4)$$

in which  $a$  and  $m$  are coefficients that characterize the relationship between formation factor ( $F$ ) and effective porosity ( $\phi_E$ ). Regression analysis of the data for these two parameters for the EBL samples, shown in Figures 3.3.1 and

3.3.2, provides values of  $m = 1.32$  and  $a = 2.1$  ( $r = -0.81$ ) for surface samples, and  $m = 2.4$  and  $a = 2.9 \times 10^{-3}$  ( $r = -0.86$ ) for the subsurface samples, where  $r$  is the correlation coefficient. The value of  $m$  for both surface and subsurface samples are close or within the range of values reported in the literature: 1.44 - 2.2 (Katsube and Hume, in prep.). The value of  $a$  for the subsurface samples is considerably smaller than the range reported in the literature of 0.6 - 3.5, but is consistent with the results of the samples from Whiteshell. The value of  $a$  for the surface samples is similar to the literature values reported for sedimentary rocks. According to Percival et al., (in prep.), mafic dyke samples appear to have lower porosities and higher formation factors whereas dendritic gabbro samples exhibit the opposite tendency. Samples of the massive gabbro show more variation. Granodiorite and syenite samples exhibit similar behaviour with respect to dendritic specimens. Percival et al. (in prep.) suggest that the values of these two parameters for the surface samples may be controlled by grain-size. The dendritic gabbro samples are mineralogically similar to the mafic dyke samples. Their differences are in grain size and texture.

The pocket porosity model (Katsube and Hume, 1986) provides a relationship between  $\phi_E$  and  $F$  which is different from that of the Archie relationship. We have

$$\phi_E = \phi_P + \tau^2(1/F) \quad (5)$$

where  $\phi_P$  is the pocket porosity and  $\tau$  is tortuosity. Contrary to the assumptions

made in equations (1) and (2), in this case it is assumed that  $\phi_p \neq 0$ . Agterberg et al., (1985) showed that it is possible to consider  $\tau$  constant for certain groups of samples. In such cases,  $\phi_p$  can be derived from equation (5) by knowing  $\phi_E$  and  $F$ . The effective porosity ( $\phi_E$ ) is plotted against  $1/F$  in Figures 3.2.3 and 3.2.4. A linear regression analysis of this data produces  $\tau = 2.21$  and  $1.80$ , and  $\phi_p = 0.11$  and  $0.054$  per cent, with a correlation factor ( $r$ ) of  $0.69$  and  $0.87$ , respectively, for surface and subsurface samples. These values are similar to those of altered granites (Agterberg et al 1985; and Katsube et al., 1985). This pocket porosity amounts to 49% and 57% of the mean values of the effective porosity of EBL surface and subsurface samples listed in Tables 3.2.1 and 3.2.2.

The relationship between the three parameters ( $\phi_E$ ,  $\tau$  and  $F$ ) with depth ( $h$ ) is shown in Figure 3.2.5. No significant correlation is seen between the two sets of parameters. The slight increase in effective porosity ( $\phi_E$ ) and decrease in formation factor ( $F$ ) with depth may be a reflection of the rock type. There is a higher content of dendritic gabbros in the shallower (0-400 m) portion of the borehole than the deeper portion (400-800 m). There is an obvious correlation between the three parameters with depth for the granite samples from the Whiteshell boreholes (Katsube and Hume, 1986), but not for the granites from Atikokan boreholes (Katsube and Hume, in prep.).

In some rocks samples a significant degree of anisotropy is seen (Table 3.2.2 and 3.2.5). According to Percival et al., (in prep.), as a result of textural considerations, dendritic gabbro samples are expected to be the most anisotropic. They consist of elongated crystals that fan out in a particular



direction. Thus, porosity and formation factor values are also assumed to be anisotropic. However, as indicated by the same authors, Tables 3.2.2 and 3.2.5 show the reverse of the expected trend. The mafic dykes show the most significant anisotropy. This is thought to be due to open hairline fractures (Percival et al in prep.). These hairline fractures could be a source of electrical conduction, thus lowering the formation factor values in the direction of the fractures. Coarser-grained dendritic gabbro samples with hairline fractures, show no obvious change in formation factor or porosity. The values are much less variable than those for mafic dyke or massive gabbro samples.

The more highly altered the plagioclase, of the surface and subsurface gabbroic samples, the higher the formation factor. Katsube et al., (1985) have shown that highly altered felsic rocks have higher formation factors and lower porosities than unaltered equivalents. The more mafic-rich felsic rocks (i.e., samples that have greater than 15% mafics) also have higher formation factor values. Thus, mafic content and degree of alteration appear to similarly effect formation factor.

The formation factor ( $F$ ) and tortuosity ( $\tau$ ) will have an effect on the diffusion rate of radionuclides if they are released from the vault. Both parameters show higher values for subsurface samples than for surface samples. This is probably due to the effect of weathering on surface samples; weathering is not likely to be significant with subsurface samples. Thus, it is formation factor and tortuosity that should be considered when discussing subsurface sample diffusion rates. The mean values of  $F$  and  $\tau$  are  $1.1 \times 10^5$  and 8.8 (Table 3.2.1), respectively, for the EBL gabbros. These are considerably higher than

those for granites, which are  $2.9 \times 10^3$  and 2.7 (Katsube and Hume, in prep.), respectively, for the granite samples from Atikokan boreholes. This implies that the diffusion rates will be much lower in the gabbros. This is a favourable characteristic from the viewpoint of radionuclide through an unfractured rock mass.

#### ACKNOWLEDGEMENTS

The authors would like to thank G.E. Larocque (CANMET) for the general guidance of this project. The authors would like to acknowledge F. Kapeller (CANMET) for guidance and the use of the drill press; F. Davis (GSC) for drafting the figures; and A. Summers (AECL) for typing the tables and drafts of this report.

REFERENCES

- Alexander, J., Hall, D.H., and Storey, B.C., 1981. Porosity measurements of crystalline rocks by laboratory and geophysical methods. Environmental Protection Unit, Institute of Geological, Harwell, ENPU-81-10, 45 p.
- Agterberg, F.P., Katsube, T.J. and Lew, S.N. 1985. Use of multiple regression for petrophysical characterization of granites as a function of alteration; in Current Research, Part B, Geol. Can., Paper 85-1B, p.451-458.
- Archie, G.E. 1942. The electrical resistivity log as an aid in determining some reservoir characteristics. Transactions of the American Institute of Mining, metallurgical and Petroleum Engineers, v. 146, p. 54-67.
- Gauvreau, C., and Katsube, T.J. 1975. Automation in electrical rock property measurements. In Report of Activities, Part A, Geological Survey of Canada Paper 75-1A, p. 83-86.
- Kamineni, D.C., McCrank, G.F., Stone, D., Ejeckam, R.B., Flindall, R. and Sikorsky, R. 1984. Geology of the central plateau of the East Bull Lake pluton, northeastern Ontario. In Current Research, Part B, Geological Survey of Canada, Paper 84-1B, p. 75-83.
- Katsube, T.J. 1981. Pore structure and pore parameters that control the radionuclide transport in crystalline rocks. Proceedings of the Technical Program, International Powder and Bulk Solids Handling and Processing, Rosemont, Illinois, p. 394-409.

Katsube, T.J., and Kamineni, D.C. 1983. Effect of alteration on pore structure of crystalline rocks: Core samples from Atikokan, Ontario. *Canadian Mineralogist*, v. 21, p. 637-646.

Katsube, T.J., Percival, J.B. and Hume, J.P. 1985. Characteristics of a rock mass by pore structure parameters. In Proceedings of the Seventh Information Meeting of the Nuclear Fuel Waste Management Program. Atomic Energy of Canada Technical Report TR-299, p. 375-413.

Katsube, T.J. and Hume, J.P. 1986. Pore structure parameters. In the Canadian Nuclear Fuel Waste Management Program: Geotechnical Studies at the Whiteshell Research Area, AECL 8410-3.

Katsube, T.J. and Hume, J.P. (in preparation). Pore structure characteristics of granitic rock samples from Atikokan research area.

Percival, J.B., Hume, J.P. and Adcock, S.W. (in preparation). Pore structure characteristics of some surface samples from East Bull Lake research area, district of Algoma, Ontario

Table 3.2.1 Minimum, maximum, mean and standard deviation (S.D.) of formation factor (F), effective porosity ( $\phi_E$ ) and tortuosity ( $\tau$ ) of EBL subsurface samples (Boreholes EBL-2 and EBL-4)

Parameter	Dendritic Gabbros	Massive Gabbros	Anorthositic Gabbros	All Gabbros	Troctolite	Units
(F)	n = 8	n = 18	n = 1	n = 27	n = 4	
Min.	30.	0.72	-	0.72	2.86	$\times 10^3$
Max.	1750.	756.	-	1750.	10.6	
G.Mean	239.	89.3	11.9	110.	5.62	
LSD	0.58	0.91	-	0.277	0.23	
( $\phi_E$ )						
Min.	0.044	0.028	-	0.028	0.027	%
Max.	0.090	0.522	-	0.522	0.068	
Mean	0.061	0.110	0.077	0.094	0.050	
S.D.	0.016	0.13	-	0.023	0.027	
( $\tau$ )						
Min.	5.19	1.79	-	1.79	1.31	
Max.	30.7	17.3	-	30.7	1.81	
G.Mean	11.9	8.1	3.03	8.75	1.59	
LSD	0.27	0.29	-	0.12	0.065	

G.Mean = geometric mean

mean = arithmetic mean

n = number of samples

LSD = log of standard deviation:

$$\log (\text{G.Mean}) = \frac{\sum \log (\text{F or } \tau)}{n}$$

Table 3.2.2 Minimum, maximum, mean and standard deviation (S.D.) of formation factor (F), effective porosity ( $\phi_E$ ), tortuosity ( $\tau$ ) and anisotropic coefficient ( $\lambda$ ) of EBL surface samples.

Parameter	Mafic Dykes	Gabbros	Syenite	Granodiorite	Units
(F)	n(N)=5(21)	n(N)=7(64)	n(N)=1(7)	n(N)=1(4)	
Min.	2.38	0.93	0.86	1.12	$\times 10^3$
Max.	301.	433.	1.82	1.85	
G.Mean	22.3	5.36	1.51	1.78	
L.S.D.	0.57	0.21	0.067	0.02	
( $\phi_E$ )	n(N)=5(16)	n(N)=7(32)	n(N)=1(3)	n(N)=1(3)	
Min.	0.039	0.053	0.425	0.508	%
Max.	0.159	0.757	0.657	0.551	
Mean	0.088	0.273	0.538	0.523	
S.D.	0.043	0.555	0.116	0.024	
( $\tau$ )	n(N)=5(21)	n(N)=7(64)	n(N)=1(7)	n(N)=1(4)	
Min.	1.92	1.31	2.70	2.94	
Max.	11.7	22.0	3.05	3.19	
G.Mean	4.17	3.50	2.82	3.02	
L.S.D.	0.22	0.058	0.026	0.015	
( $\lambda$ )	n(N)=5(7)	n(N)=7(22)	n(N)=1(3)	n(N)=1(1)	
Min.	1.56	1.00	1.02		
Max.	45.8	49.2	1.32		
Mean	10.1	5.38	1.21	1.05	
S.D.	16.02	2.44	0.07		

G.Mean = geometric mean

Mean = arithmetic mean

n(N) = number of samples (number of specimens or measurements)

L.S.D. = log of standard deviation:

$$\log (\text{G.Mean}) = \frac{\sum \log (\text{F or } \tau)}{n} \pm (\text{L.S.D.})$$



Table 3.2.3 Pore Structure Parameters for EBL Standard Samples

Sample Number		F	$\phi_E$	$\tau$	Rock Type	
EBL-2	-2.8	376.00	0.079	17.26	GB	(D)
	-29.9	115.00	0.056	8.015	GB	(D)
	-69.4	2.86	0.081	1.520	TR	
	-79.4	6.29	0.027	1.310	TR	
	-130.5	95.50	0.068	8.031	TR	
	-147.3	264.00	0.046	11.006	GB	(M)
	-173.9	69.60	0.059	6.421	GB	(M)
	-201.4	589.00	0.034	14.209	GB	(M)
	-239.57	1750.00	0.054	30.667	GB	(D)
	-272.68	30.00	0.090	5.085	GB	(D)
	-298.7	137.00	0.049	8.222	GB	(D)
	-342.46	1.71	0.188	1.794	GB	(M)
	-372.7	205.00	0.105	14.668	GB	(M)
	-419.83	2.90	0.343	3.154	GB	(M)
	-547.9	11.90	0.077	3.025	GB	(M)
	-613.4	147.00	0.038	7.505	GB	(M)
	-692.85	31.00	0.093	5.371	GB	(M)
-733.7	48.10	0.185	9.433	GB	(M)	
-767.1	0.72	0.522	1.940	GB	(M)	
-804.1	139.00	0.065	9.154	GB	(M)	
EBL-4	-24.9	124.00	0.079	9.870	GB	(M)
	-36.9	425.00	0.055	15.336	GB	(D)
	-57.5	81.30	0.062	7.123	GB	(D)
	-122.9	10.60	0.029	1.760	TR	
	-150.12	5.10	0.064	1.808	TR	
	-206.8	676.00	0.044	17.304	GB	(M)
	-251.0	756.00	0.037	16.700	GB	(M)
	-298.2	459.00	0.041	13.753	GB	(M)
	-325.0	462.00	0.028	11.458	GB	(M)
	-376.4	422.00	0.032	11.609	GB	(M)

UNITS (x10<sup>3</sup>) (%)

- F = formation factor
- $\phi_E$  = effective porosity
- $\lambda$  = tortuosity
- GB = Gabbro
- TR = Dendritic
- M = Massive
- A = Anorthositic

Table 3.2.4 Pore Structure Parameters for EBL Surface Samples

SAMPLE NUMBER	F	$\Phi_E$	$\tau$	Rock Type	
1-A-3	3.82	0.119	2.133	Mafic Dyke (Black Dyke)	
1-A-6	20.60		4.947		
1-C-3	6.87	0.104	2.673		
1-C-5	12.90		3.657		
1-C-9	13.20		3.708		
1A-A-3	18.70	0.056	3.231		
2-A-5	110.00	0.053	7.648		Metagabbro (M)
2-B-1	8.80	0.067	2.423		
2-C-1	433.00	0.112	22.034		
2-C-3	116.00		11.389		
2A-B-1	2.89	0.201	2.408		
2A-C-1	20.60	0.082	4.125		
2A-C-3	258.00		14.568		
3-A-4	104.00	0.042	6.632	Mafic Dyke (Green Dyke)	
3-B-1	11.80	0.141	4.071		
4-A-5	1.70	0.508	2.939		
4-B-1	1.85	0.551	3.191		
4-B-3	1.12		2.485		
4-C-1	1.76	0.511	3.001		
5-A-1	1.82	0.425	2.778	Syenite	
5-A-3	1.81		2.772		
5-A-7	1.34		2.382		
5-B-1	1.38	0.531	2.704		
5-B-5	1.27		2.596		
5-C-1	1.41	0.657	3.048		
5-C-4	0.863		2.381		
6-A-1	2.67	0.425	3.370		Metagabbro (M)
6-A-3	2.35		3.159		
6-B-1	2.22	0.444	3.140		
6-C-1	5.77	0.271	3.955		
6-C-3	2.81		2.762		
7-A-1	4.32	0.405	4.183	Metagabbro (M)	
7-A-5	2.70		3.306		
7-A-9	2.75		3.335		
7-B-1	7.42	0.395	5.412		
7-B-4	11.10		6.627		
7-B-6	3.77		3.857		
7-C-1	3.23	0.264	2.919		
7-C-5	2.67		2.653		
7-C-7	1.85		2.210		

Table 3.2.4 (continued)

SAMPLE NUMBER	F	$\phi_E$	$\tau$	Rock Type
8-A-1	2.25	0.433	3.122	Metagabbro (Anorthositic)
8-B-1	3.22	0.343	3.322	
9-A-3	9.31	0.114	3.258	Mafic Dyke (Nipissing Diabase)
9-B-1	30.90	0.0786	4.926	
9-B-4	45.40		5.972	
10-A-3	109.00	0.043	6.874	Mafic Dyke (Nipissing) Diabase)
10-B-1	3.56	0.103	1.915	
10-B-3	2.38		1.566	
10-C-1	6.12	0.116	2.664	Metagabbro (M)
11-A-1	1.70	0.101	1.310	
11-A-2	3.36		1.842	
11-A-3	21.00		4.609	
11-A-7	5.01		2.249	
11-A-9	30.80		5.579	
11-B-1	2.11	0.095	1.418	
11-B-3	10.20		3.116	
11-B-7	4.54		2.080	
11-C-1	11.70	0.235	5.241	
11-C-3	4.86		3.381	
11-C-6	7.42		4.176	
12-A-1	3.00	0.430	3.591	Metagabbro (M)
12-A-5	3.30		3.768	
12-B-1	5.75	0.256	3.837	
12-B-5	18.90		6.933	
12-C-1	5.12	0.316	4.022	
12-C-5	5.30		4.093	
13A-A-1	2.44	0.259	2.521	Metagabbro (D)
13A-A-5	1.98		2.265	
13A-B-1	2.92	0.254	2.725	
13A-B-3	2.21		2.372	
13A-B-7	2.19		2.357	
13A-C-1	2.59	0.241	2.496	
13A-C-3	1.93		2.154	
13A-C-7	1.850	0.241	2.109	
13B-A-1	4.33	0.214	3.046	
13B-A-2	4.21		3.002	
13B-B-1	4.13	0.238	3.134	
13B-C-1	2.15	0.366	2.802	
13C-A-1	1.62	0.312	2.247	
13C-A-3	2.01		2.503	
13C-B-1	1.62	0.757	3.504	
13C-B-3	1.47		3.341	
13C-C-1	0.932	0.365	1.844	

Table 3.2.4 (continued)

SAMPLE NUMBER	F	$\phi_E$	$\tau$	Rock Type
13C-C-2	0.980		1.891	
13D-A-1	4.11	0.255	3.237	
13C-A-5	1.85		2.169	
13D-B-1	9.48	0.172	4.039	
13D-B-5	9.57		4.057	
13D-C-1	1.28	0.260	1.824	
13D-C-5	1.70		2.100	
14-A-1	30.60	0.0509	3.946	Mafic Dyke
14-A-5	15.60	0.151	4.847	(Black Dyke)
14-B-2	27.60	0.159	6.628	
14-B-6	301.00	0.045	11.659	
14-C-1	19.60	0.044	2.923	
14-C-5	121.00	0.0389	6.849	
Units	( $\times 10^3$ )	(%)		

F = formation factor

$\phi_E$  = effective porosity

$\tau$  = tortuosity

Table 3.2.5 Coefficient of anisotropy ( $\lambda$ ) for EBL surface samples

Sample	Rock Type	F(x10 <sup>3</sup> )		Sample	Rock Type	F(x10 <sup>3</sup> )	
1-C-3	Maffie Dyke	6.87	1.79	11-B-1	Gabbro	2.11	1.24
1-A-3	(BD)	3.82		11-A-1	(m)	1.70	
2-C-1	Gabbro	433.00	49.20	11-C-1	Gabbro	11.70	5.55
2-B-1	(m)	8.80		11-B-1	(m)	2.11	
2A-C-1	Gabbro	20.60	7.13	12-B-1	Gabbro	5.75	1.92
2A-B-1	Gabbro	2.89		12-A-1	(m)	3.00	
3-A-4	Maffie Dyke	104.00	3.81	12-B-1	Gabbro	5.75	1.12
3-B-1	(GD)	11.80		12-C-1	(m)	5.12	
4-B-1	Granodiorite	1.85	1.05	13A-B-1	Gabbro	2.92	1.19
4-C-1		1.76		13A-A-1	(D)	2.44	
5-A-1	Syenite	1.82	1.32	13A-C-1	Gabbro	2.59	1.06
5-B-1		1.38		13A-A-1	(D)	2.44	
5-A-1	Syenite	1.82	1.29	13A-B-1	Gabbro	2.92	1.13
5-C-1		1.38		13B-B-1	(D)	4.13	
6-A-1	Gabbro	2.67	1.20	13B-A-1	Gabbro	4.33	2.01
6-B-1	(m)	2.22		13B-C-1	(D)	2.15	
6-C-1	Gabbro	5.77	2.16	13C-A-1	Gabbro	1.62	1.0
6-A-1	(m)	2.67		13C-B-1	(D)	1.62	
7-B-1	Gabbro	7.42	1.72	13C-A-1	Gabbro	1.62	1.74
7-A-1	(m)	4.32		13C-C-1	(D)	0.932	
7-A-1	Gabbro	4.32	1.34	13D-B-1	Gabbro	9.48	2.31
7-C-1	(m)	3.23		13D-A-1	(D)	4.11	
7-B-1	Gabbro	3.22	1.43	13D-B-1	Gabbro	9.48	7.41
7-C-1	(m)	3.23		13D-C-1	(D)	1.28	
8-B-1	Gabbro	3.22	1.43	13D-B-1	Gabbro	9.48	7.41
8-A-1	(A)	2.25		13D-C-1	(D)	1.28	
9-B-1	Maffie Dyke	30.90	3.32	14-A-1	Maffie Dyke	30.60	1.56
9-A-3	(ND)	9.31		14-C-1	(BD)	19.60	
10-A-3	Maffie Dyke	109.00	45.79	14-C-5	Maffie Dyke	121.00	7.76
10-B-3	(ND)	2.38		14-A-5	(BD)	15.60	
10-C-1	Maffie Dyke	6.12	1.72				
10-B-1	(ND)	3.56					

BD = blocks dyke  
 GD = Green dyke  
 ND = Nipissing diabase

M = massive gabbro  
 A = anorthositic gabbro  
 D = dendritic

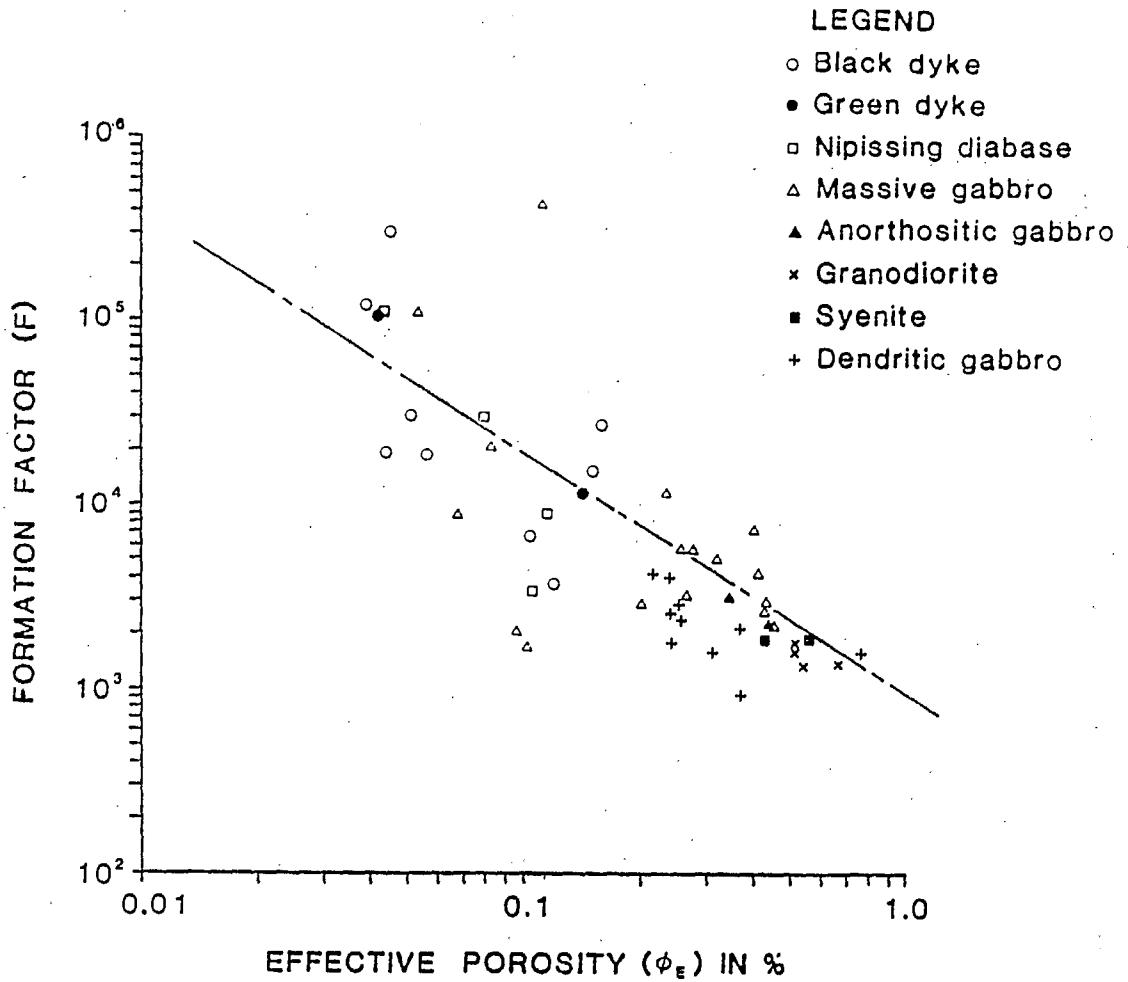


Figure 3.2.1 Formation factor (F) as a function of effective porosity ( $\phi_E$ ): the Archie Relationship for East Bull Lake surface samples (after Percival, et al., in prep.).

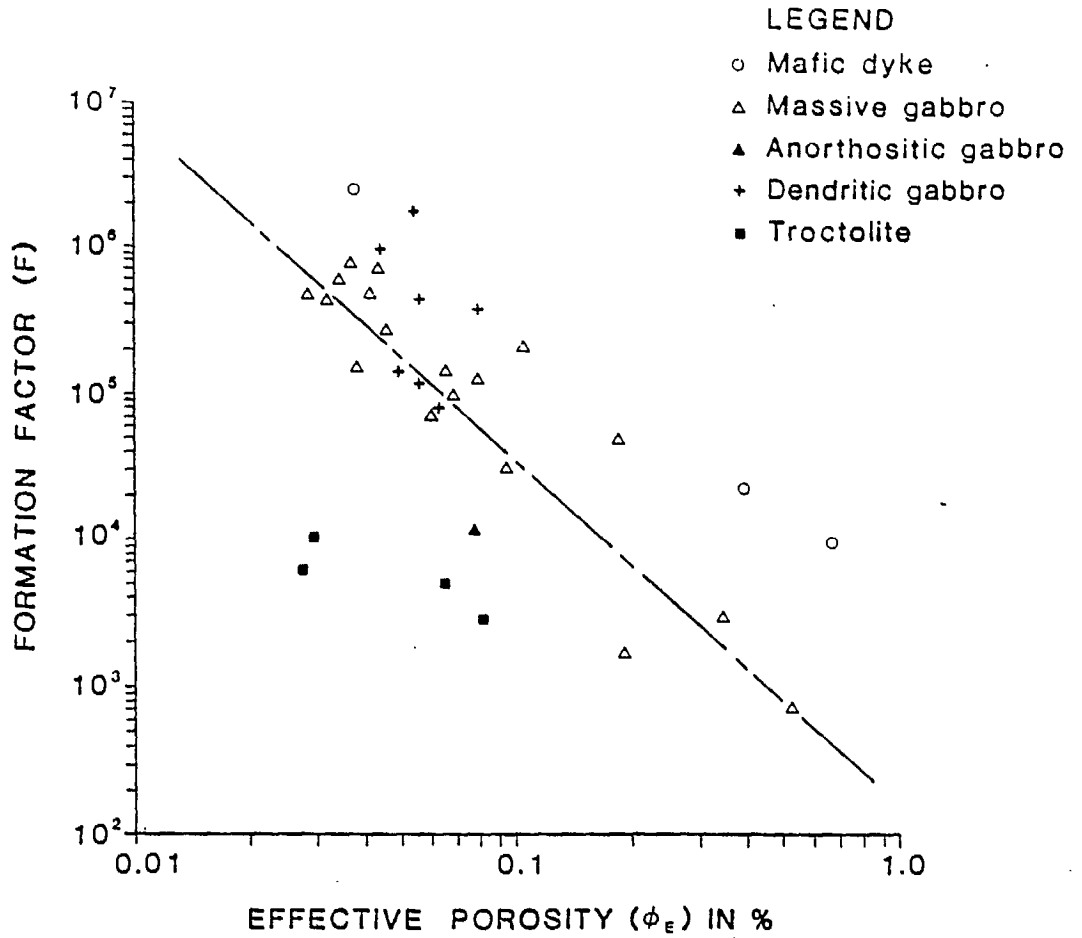


Figure 3.2.2 Formation factor (F) as a function of effective porosity ( $\phi_E$ ): the Archie Relationship for East Bull Lake subsurface samples (after Percival, et al., in prep.).

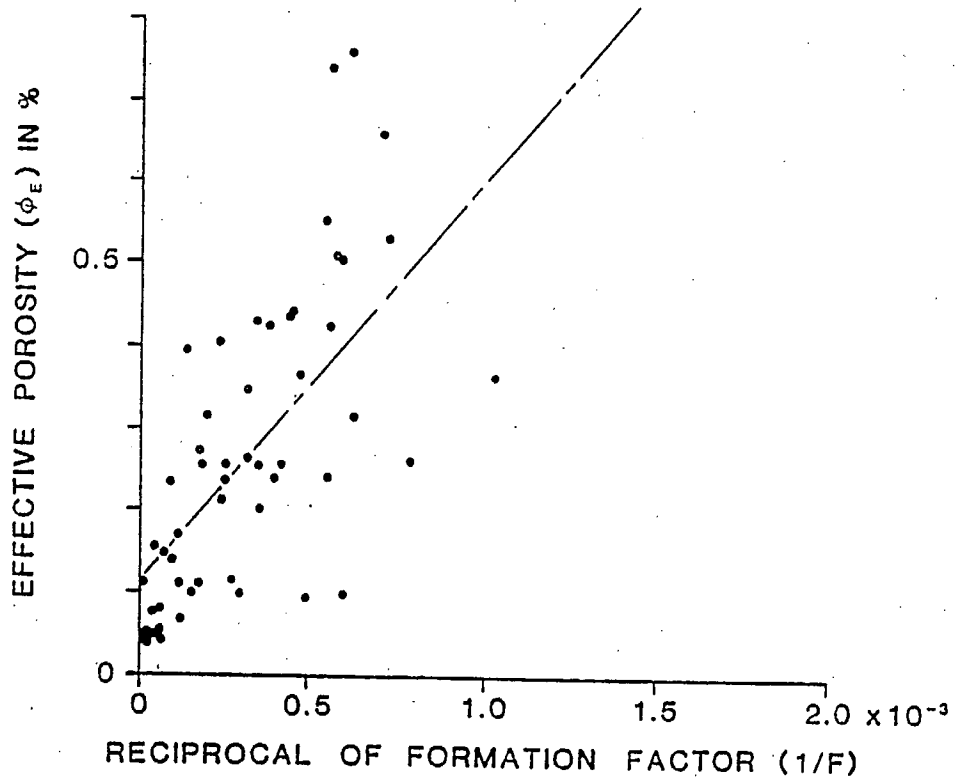


Figure 3.2.3 Effective porosity ( $\phi_E$ ) as a function of the reciprocal of the formation factor ( $1/F$ ) for East Bull Lake surface samples:

$$\phi_E = 1.1 \times 10^{-3} + 4.9 (1/F)$$



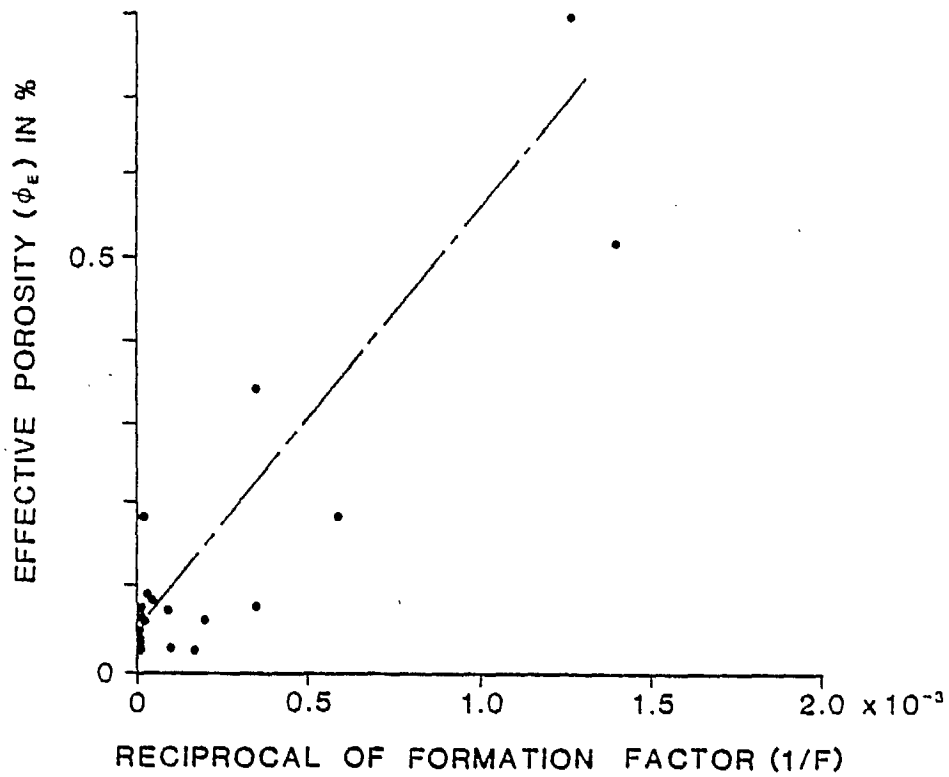


Figure 3.2.4 Effective porosity ( $\phi_E$ ) as a function of the reciprocal of the formation factor ( $1/F$ ) for East Bull Lake subsurface samples:

$$\phi_E = 5.4 \times 10^{-4} + 3.23 (1/F).$$

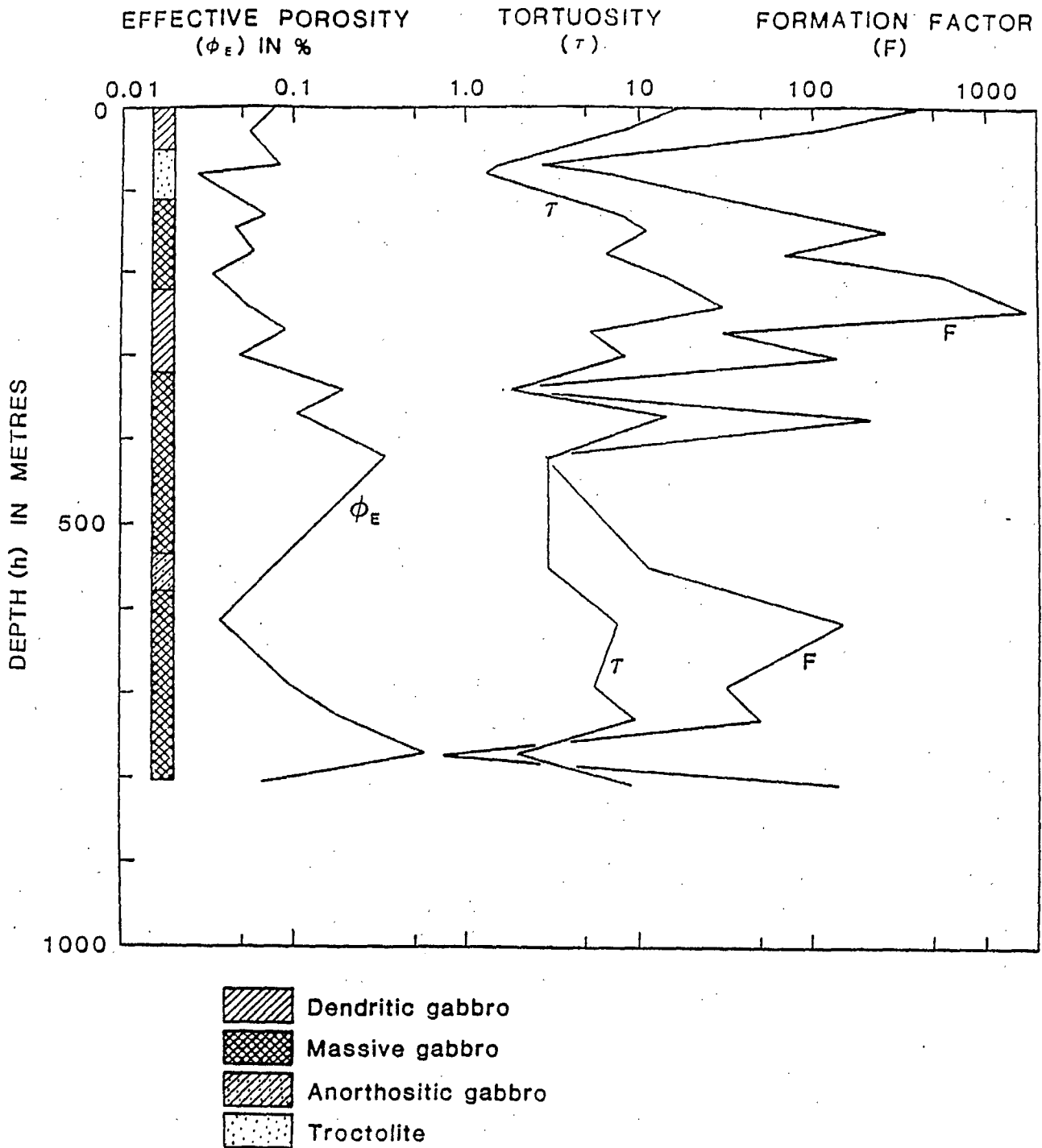


Figure 3.2.5 Formation factor ( $F$ ), tortuosity ( $\tau$ ) and effective porosity ( $\phi_E$ ) as a function of depth ( $h$ ) for samples from borehole EBL-2.

3.3

THERMAL PROPERTIES

Malcolm Drury

Lithosphere and Canadian Shield Division

Geological Survey of Canada

1, Observatory Crescent

Ottawa, Ontario

K1A 0Y3

3.3.1 Introduction

Measurements of thermal conductivity and diffusivity were made at ambient temperature on 88 samples from borehole EBL-3, at the former Earth Physics Branch, and are described in Drury (1986). Measurements of conductivity and diffusivity were made on the same water-saturated discs of the above.

3.3.2 Results

88 conductivity and 87 diffusivity measurements were made, along with porosity and density. The data are given in the Appendix 3.3.1. Figs. 3.3.1 and 3.3.2 show the variation of conductivity and diffusivity with depth. From these measurements specific heat was calculated. There appears to be some correlation between thermal properties and the gabbro anorthosite boundary. Within individual lithological units there is wide variation in both properties. Figs. 3.3.3 and 3.3.4 show the data in histogram form. The wide variation in thermal diffusivity is highlighted by this type of plot.

REFERENCE

Drury, M.J. 1986. Thermophysical properties of rock samples from WNRE and URL boreholes. AECL NFWMP level 2 rept.

TABLE 3.3.1. Mean and standard deviations of measured low temperature thermal conductivity, thermal diffusivity and specific heat.

Property	Mean	S.D.	Units	Number
Conductivity	2.55	0.72	W/m.K	88
Diffusivity	0.95	0.23	mm <sup>2</sup> /S	87
Specific heat	1080	194	J/kg.K	87

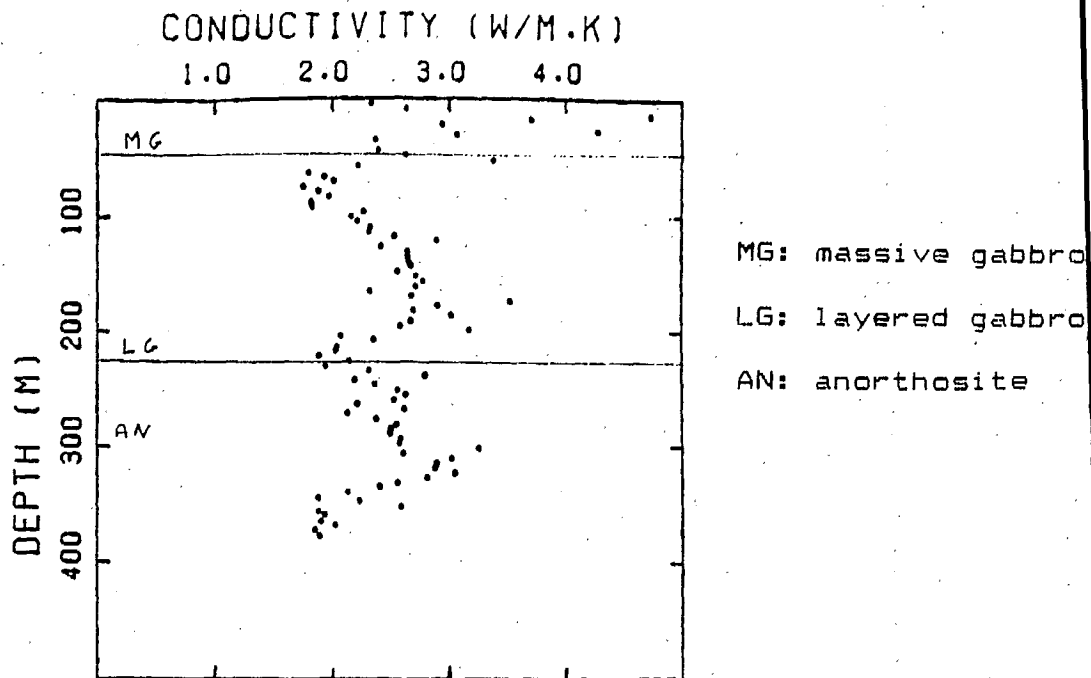


Fig. 3.3.1 Variation with depth of thermal conductivity of EBL samples.

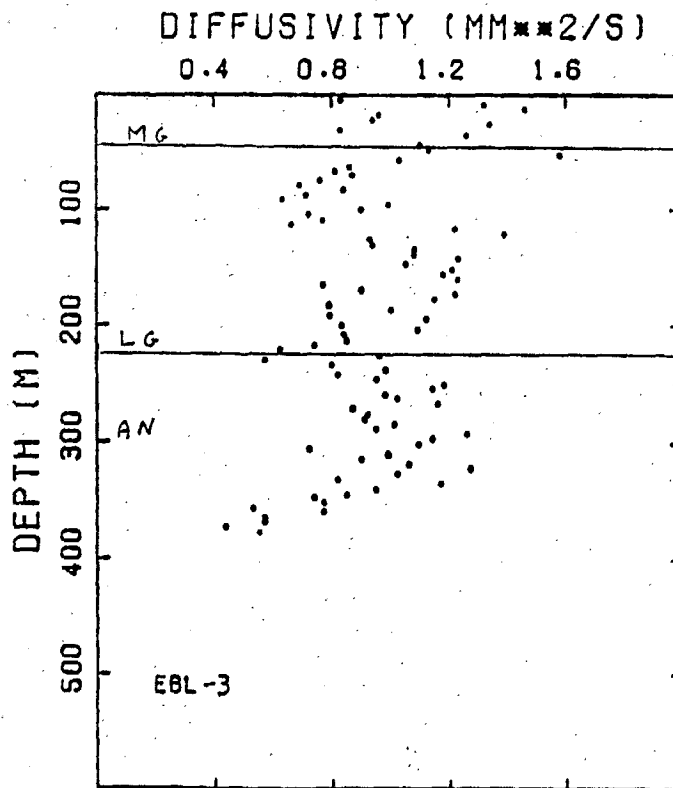


Fig. 3.3.2 Variation with depth of thermal diffusivity.

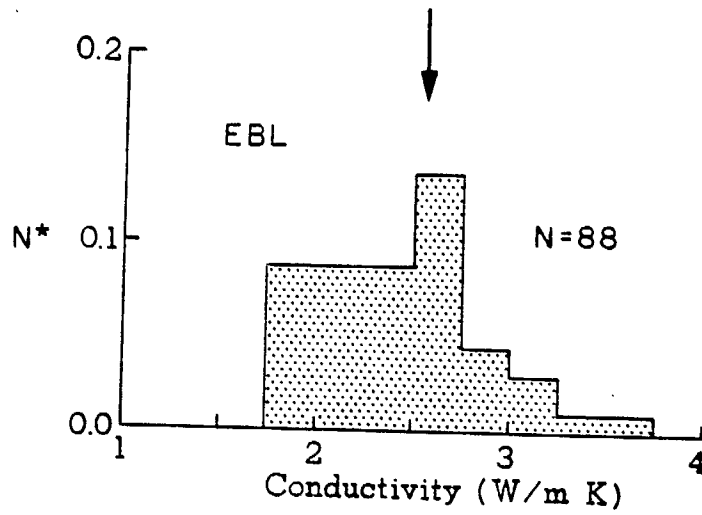


Fig. 3.3.3 Histogram distribution of low temperature thermal conductivity data of East Bull Lake borehole samples. N is the number of samples and N\* is the number of samples per interval normalised to N. Arrow indicates arithmetic mean.

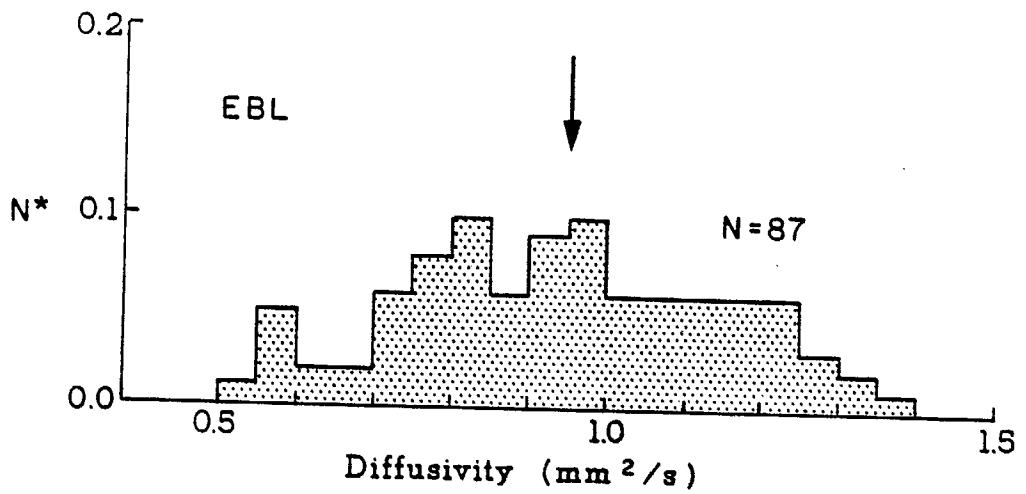


Fig. 3.3.4 As Fig. 3.3.3 for thermal diffusivity.

APPENDIX 3.3.1

Conductivity, diffusivity, density and porosity data for EBL-3 samples.

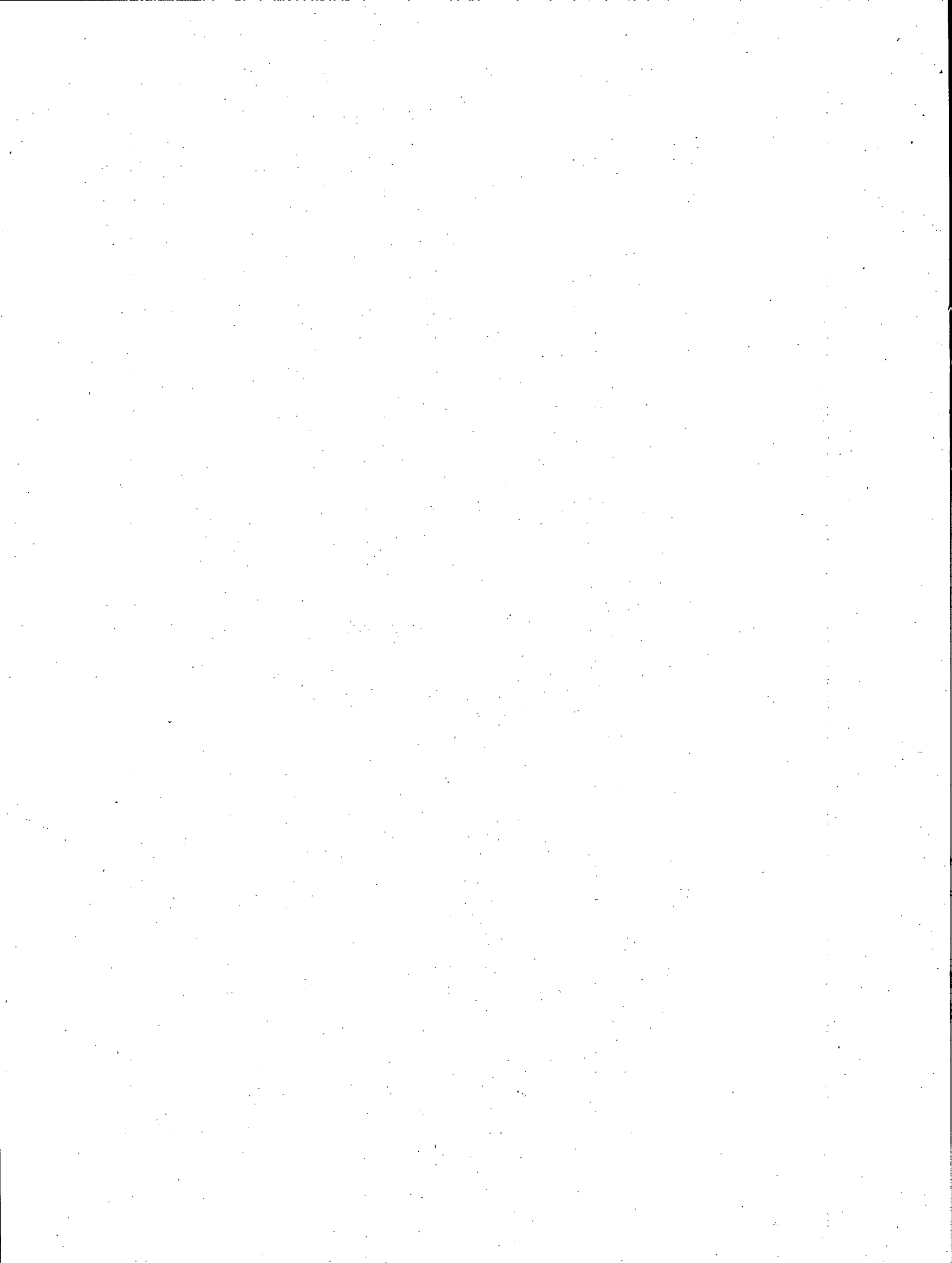
Depth(m)	Cond W/m.K	Diff mm <sup>2</sup> /S	Dens Mg/m <sup>3</sup>	Por
4.4	2.33	.83	2.89	.004
8.7	2.63	1.32	2.88	.003
13.1	4.73	1.46	2.82	.004
17.2	3.70	.96	2.80	.002
21.8	2.94	.94	2.82	.001
26.0	4.28	1.34	2.80	.006
30.4	3.07	.83	2.82	.0154
34.9	2.37	1.26	2.76	.011
39.3	7.17	—	2.65	.005
43.6	2.39	1.10	2.79	.008
47.9	2.62	1.13	2.82	.004
52.2	3.38	1.58	2.78	.016
56.6	2.22	1.03	2.68	.019
62.3	1.80	.86	2.84	.022
65.8	1.93	.81	2.84	.011
69.6	2.01	.87	2.86	.008
73.9	1.75	.76	2.77	.021
78.2	1.88	.69	2.84	.014
86.8	1.82	.71	2.82	.028
91.1	1.83	.63	2.82	.015
95.6	2.26	.99	2.85	.014
100.1	2.16	.90	2.87	.011
103.9	2.21	.72	2.88	.008
108.6	2.32	.77	2.89	.008
112.9	2.31	.66	2.87	.009
117.2	2.52	1.22	2.80	.008
121.3	2.89	1.39	2.81	.006
125.8	2.41	.93	2.83	.015
130.5	2.64	.94	2.86	.009
134.4	2.64	1.08	2.83	.004
139.1	2.65	1.08	2.85	.004
142.9	2.67	1.23	2.83	.007
147.1	2.55	1.05	2.79	.007
151.6	2.71	1.21	2.81	.006
155.8	2.77	1.18	2.88	.008
160.3	2.71	1.23	2.84	.004
164.5	2.32	.77	2.73	.007
168.7	2.67	.90	2.79	.007
173.2	3.52	1.22	2.91	.017
177.2	2.90	1.15	2.90	.004
181.4	2.69	.79	2.86	.010
185.8	3.02	1.00	2.97	.006



APPENDIX 3.3.1. (continued)

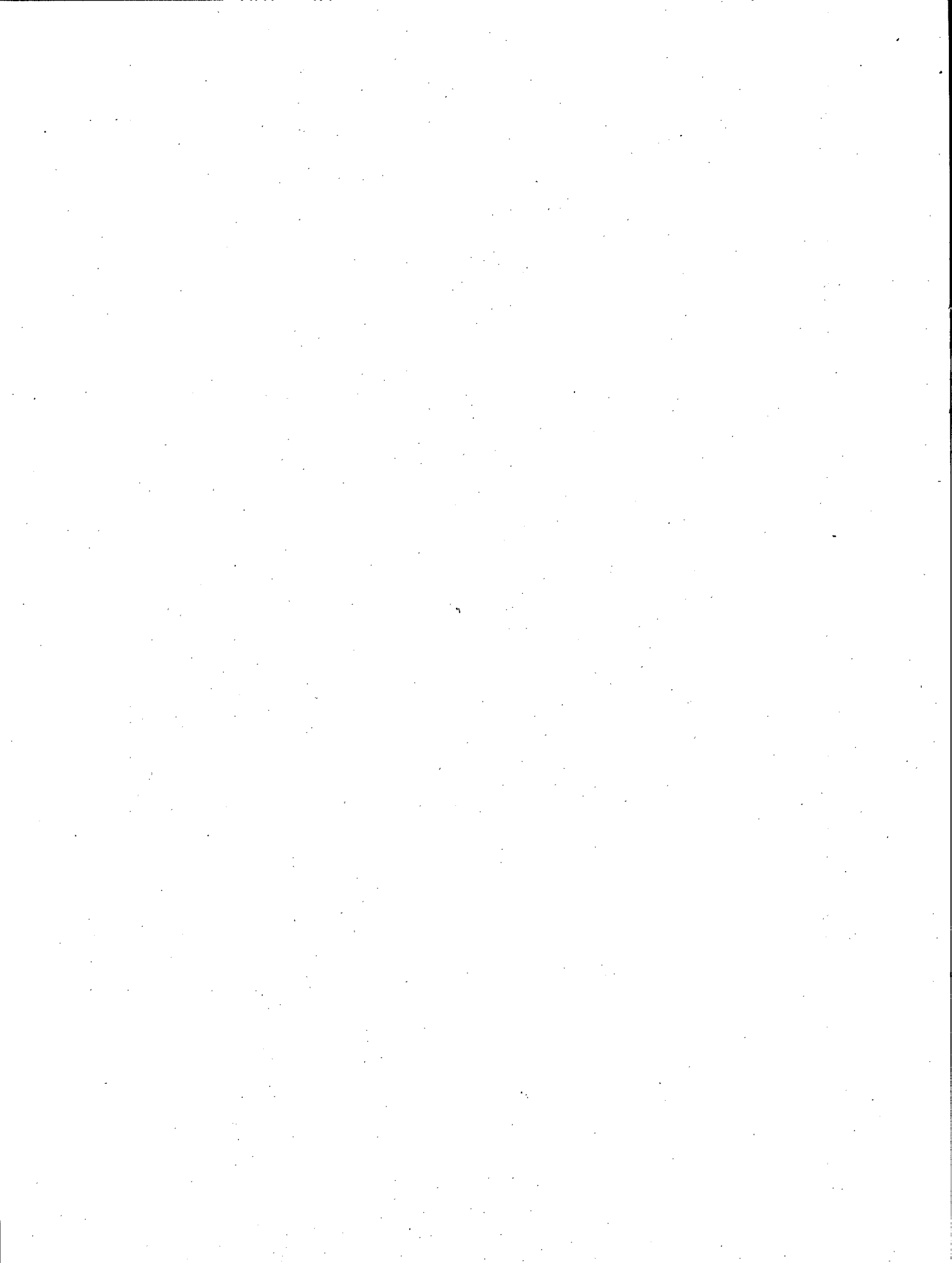
Conductivity, diffusivity, density and porosity data for EBL-3 samples.

Depth(m)	Cond W/m.K	Diff mm <sup>2</sup> /S	Dens Mg/m <sup>3</sup>	Por
190.4	2.67	.79	2.82	.005
194.4	2.58	1.12	2.86	.009
198.8	3.17	.83	2.90	.008
203.0	2.07	1.09	2.90	.023
206.9	2.35	.84	2.85	.027
212.2	2.04	.85	2.88	.012
216.1	2.03	.74	2.88	.017
220.5	1.89	.62	2.86	.022
229.0	1.94	.57	2.90	.013
232.9	2.31	.80	2.89	.012
237.4	2.79	.98	2.45	.004
241.4	2.19	.82	2.70	.006
245.6	2.36	.95	2.70	.006
250.5	2.55	1.18	2.97	.001
254.2	2.62	1.14	2.79	.007
258.6	2.52	.98	2.74	.006
262.4	2.21	1.02	2.76	.001
266.8	2.61	1.16	2.86	.011
270.4	2.13	.87	2.80	.005
275.3	2.37	.92	2.72	.022
279.8	2.54	.91	2.90	.003
283.6	2.49	1.01	2.92	.002
287.9	2.49	.95	2.80	.014
292.2	2.58	1.26	2.83	.012
296.4	2.57	1.14	2.86	.005
300.7	3.25	1.09	2.95	.004
304.8	2.60	.72	2.90	.008
309.2	3.02	.99	2.92	.003
313.4	2.89	.90	2.89	.002
317.7	2.88	1.06	2.86	.004
321.8	3.05	1.27	2.78	.010
325.8	2.81	1.02	2.76	.003
330.6	2.55	.82	2.80	.003
334.2	2.40	1.17	2.79	.002
339.0	2.13	.95	2.84	.012
343.7	1.88	.85	2.86	.014
346.7	2.23	.74	2.87	.014
350.8	2.58	.77	2.89	.015
355.6	1.88	.53	2.82	.028
358.4	1.93	.77	2.81	.035
364.0	1.90	.57	2.74	.051
367.9	2.02	.57	2.64	.050
371.7	1.85	.44	2.80	.016
376.8	1.89	.55	2.77	.036



CHAPTER 4

GEOPHYSICAL PROPERTIES



4.1

MAGNETIC PROPERTIES

A.G. Latham\*, W.A. Morris\*\*, P. Lapointe\*, and K.L. Harding\*

\*: Geomagnetic Laboratory,  
Geological Survey of Canada  
601 Booth Street  
Ottawa, Ontario  
K1A 0E8

\*\* : Morris Magnetics,  
R.R.#2  
Lucan, Ontario  
NOM 2J0

4.1.1 Introduction

This report summarises the analyses and interpretation of the magnetic properties of EBL borehole and surface samples. Most of the interpretation is concerned with distinguishing between primary lithological units, intrusions and

degrees of severity of alteration associated with fracture zones. Step changes in bulk magnetic susceptibility (BMS) in the core log are mostly associated with lithological changes, and low BMS troughs are usually associated with alteration around zones of dense fracturing. The recognition of lithological zones and of degrees of alteration is greatly aided by the use of the BMS and fracture histograms, and by plotting the BMS distributions, on a log scale, against cumulative frequency, (Lapointe et al, 1986).

#### 4.1.2 Concepts

Bulk magnetic susceptibility is the ease with which a rock becomes magnetized in a low magnetic field, and it is a function, in the first instance, of the concentration of titanomagnetite in the sample. The BMS of unaltered rock possesses a characteristically high level. Hematite, the common weathering product of magnetite (and of other ferromagnesian minerals), has a susceptibility which is a factor of about 1000 lower than magnetite (Telford et al, 1976). Consequently, the measurement of low susceptibility from a borecore usually distinguishes the low-temperature alteration zones from the fresh, unaltered rock.

The susceptibility of titanomagnetite decreases with increasing grain size, and varies in a more complicated way with titanium content (Day, 1977). In the EBL layered gabbro, the magnetic oxides occur in low concentrations as unexsolved titanomagnetite grains of sizes around 1 mm and as fine needles of magnetite

along the cleavage planes of pyroxene grains (Lapointe et al, 1983). In the EBL gabbro it is probably valid to attribute most levels of BMS with a distinct lithological layer or layers.

Morris (1984) reported remanence measurements from the outcrop as aids to the lithological and alteration work. These measurements have also been used in the interpretation of magnetic anomaly mapping, but this aspect will not be discussed here.

#### 4.1.3 Instrumentation and methodology

Magnetic susceptibility of the EBL-1 to -4 borecores was measured using a Bison susceptibility bridge and a Sapphire Instruments susceptibility meter SI-2 with measurements taken;

- (1) at 10 cm intervals down the core,
- (2) on the surface outcrop in situ, and on shallow 15 cm cores. (Lapointe et al, 1984).

#### 4.1.4 Data analysis and presentation

The BMS, as reported in Morris, (1984), Lapointe et al, (1983) and Morris et al (1984), were plotted (a) as raw data against depth, (b) as histograms of  $\log_{10} X$ , and (c) as plots of  $\log_{10} X$  versus cumulative frequency.

In this report, plots of BMS versus borehole depth have been plotted along with density, lithology and fracture density, for comparative and correlative purposes.

#### 4.1.5 Demarcation of susceptibility levels

##### NB Notation and Phraseology

The following word usage may be noted:

Alteration is the change of a primary mineral assemblage by secondary processes such as hydrothermal or weathering processes. It may be defined qualitatively in terms of; secondary mineral assemblages, as is common in petrography; by colour changes; by the presence of fracture infilling minerals or, as in this report, by a decrease in BMS caused by the oxidation of magnetite.

Level denotes a BMS mean that is characteristic of lithology or of alteration.

Degree or Severity of alteration is judged by the level to which the BMS has been lowered; or elsewhere, by colour changes, etc.

Extent of alteration is used loosely to denote the combination of the severity and the spatial presence of alteration.

Zone refers to an interval in a borecore that is characterized by a given lithology, fracture sequence, or level of BMS, etc.

Susceptibility tends to show a log normal distribution about its mean; that is, if  $\log_{10} x$  is plotted against cumulative frequency (on a probability scale), then the BMS characteristic of that lithology shows a straight line segment whose mean and variance may then be estimated. This approach helps to establish the methodology for the recognition and demarcation of levels of BMS due either to lithological changes or to degrees of rock alteration.



#### 4.1.6 Results and interpretation

This report covers the four East Bull Lake boreholes EBL-1,2,3 and 4. Detailed lithology and fracture logs have been presented by Ejeckam et al (1985). A summary of the lithology and the variations in BMS are presented in figures 4.1.1 and 4.1.2. Figures 4.1.3 to 4.1.6 show the addition of the fracture logs.

It is apparent, first of all, that most of the levels and changes in level are controlled by lithology. Examples are;

- 1) increases in BMS in the magnetite-rich troctolite seen in EBL-1 and -2, and in the magnetite-rich zone of EBL-3.
- 2) increases in BMS in some amphibolite veins such as in EBL-1 at about 380 m.
- 3) low levels of BMS observed in the anorthosites, except for the magnetite-richer layers in EBL-3.

An attempt has been made to separate out the effects of alteration on BMS by plotting BMS histograms and their log cumulative plots. These are presented in figures 4.1.7 to 4.1.11, and are now briefly discussed:

1) Gabbro,

- (a) The gabbro occurs in three separate units in EBL-1 which together yield an almost perfect log-normal distribution with a mean about  $8 \cdot 10^{-4}$  SI.
- (b) EBL-2 has both a more magnetite-rich layer (depth extent about 170-190 m) and more fracturing, the latter having induced the lower BMS values. The BMS histogram is principally bimodal, and corresponds to two approximately log-normal distributions. One of these probably corresponds to that seen in EBL-1, though its mean is slightly lower

at  $7 \cdot 10^{-4}$  SI.

- 2) Amphibolite veins (figure 4.1.9). These, taken together, show only an approximate log-normal distribution, reflecting varying concentrations of magnetite, vein to vein. They appear to have suffered little alteration.
- 3) Anorthosite. The anorthosite layers show a close approximation to a log-normal distribution of BMS. Low BMS spikes especially in EBL-4 may be evidence for the effect of fracture-bearing groundwater.
- 4) Magnetite-rich units (figures 4.1.10 and 4.1.11). These were combined from the troctolite and anorthosite units. Besides the different populations present, fracturing has lowered some BMS levels by about two orders of magnitude in boreholes EBL-1, -2 and -3, testifying to the severity of alteration.

#### 4.1.7 Fracture - Induced Alteration

Where there are fractures, these tend to lower the BMS giving a spikey trace in the log; the loss of magnetite and titanomagnetite, reflected in the lowering of BMS, is due to the flow of water in the fractures. Generally, the depth of the spike (trough) reflects the degree of alteration, as was also the case for the Lac du Bonnet and Eye-Dashwa Lakes granites. BMS levels below about  $10^{-4}$  SI approach the level of sensitivity of the instrument and essentially register the complete loss of magnetite.

Figures 4.1.3 to 4.1.6 show, however, that an increase in fracture frequency (fractures per meter) does not always correspond to a drop in BMS (eg. in EBL-2 from 570 m to 610 m). There are two reasons for this;

- 1) Where magnetite-rich dykes have invaded the country rock, and fractures have developed within, and adjacent to the dyke, BMS has locally increased rather than decreased. e.g. The four dykes in ELB-2 between 210m and 255, (figure 4).
- 2) Where serpentinization has increased the magnetite content of the country rock then, although the rock may subsequently have been fractured, nevertheless the BMS shows an increase, e.g. the two generations of serpentinite in the troctolite unit (McCrank et al, 1985).

#### 4.1.8 Conclusions

The levels and changes in BMS in the borecores of the East-Bull Lake gabbro correlate very well with the changes in lithology. Although it is recognized that fracture - induced alteration also lowers BMS, such effects are not always obvious in the four logs presented here, and in fact, some fractures associated with veins may even show an increase in BMS. From the point of view of making a rapid assessment of degrees of alteration associated with different fracture zones, the interpretation of BMS of this type of body must be made with care, and may not be unique. In general the little alteration associated with many fractures appear to be due to the relatively low porosity and permeability of the surrounding rock matrix.

REFERENCES

- Chomyn, B.A., Lapointe, P., Morris, W.A. and Coles, R.L. 1985. Magnetic susceptibility applications in Borehole Geophysics. Canadian Exploration Geophysical Society/Geological Survey of Canada Symposium/Spec. Pub of GSC. (ed) P. Killeen.
- Chomyn, B.A., Morris, W.A., Lapointe, P. and Coles, R.L. 1985. Applications of magnetic susceptibility to assessing the degree of alteration of crystalline rock. The Geoscience Program - Proceedings of the Seventeenth Information Meeting of the Nuclear Fuel Waste Management Program. AECL Technical Record, TR - 299, 609-621.
- Day, R. 1977. TRM and its variation with grain size: A review. Advances in Earth and Planetary Sciences, 1, 1-33.
- Ejeckam, R.B., Sikorsky, R.I., Kamineni, D.C. and McCrank, G.F.D., 1985. Subsurface geology of the East Bull Lake research area (RA 7) in northeastern Ontario, AECL Technical Record, TR-348.
- Lapointe, P., Morris, W.A., and Harding, K.L. 1986. Interpretation of magnetic susceptibility; a new approach to the geophysical evaluation of the degree of rock alteration. Canadian Journal of Earth Sciences, 23, 393-401.
- Lapointe, P., Chomyn, B.A., and Morris, W.A. Annual Report 1982-1983. Rock Magnetic Properties Task, Earth Physics Branch. File 83-4.

- McCrank, G.F.D., Stone, D., Ejeckam, R.B., Kamineni, R.I., Sikorsky, R.I., and McEwen, J. 1985. Surface and subsurface geological investigations of the East Bull Lake pluton, Research area 7. In the Geoscience Program - Proceedings of the Seventeenth Information Meeting of the Nuclear Fuel Waste Management Program. TR-229.
- Morris, W.A., 1984. Rock Magnetic Studies at RA-7. The East Bull Lake gabbro anorthosite. 1984 Internal Report, Earth Physics Branch.
- Morris, W.A., Lapointe, P., Chomyn, B.A., and Balch, K.L. Annual Report 1983-1984 Rock Magnetic Properties Task, Earth Physics Branch. File 84-20.
- Telford, W.M., Geldart, L.P., Sheriff, R.E. and Keys, D.A. 1976. Magnetic susceptibilities of various minerals, table 3, in Applied Geophysics, Cambridge University Press. pp 860.

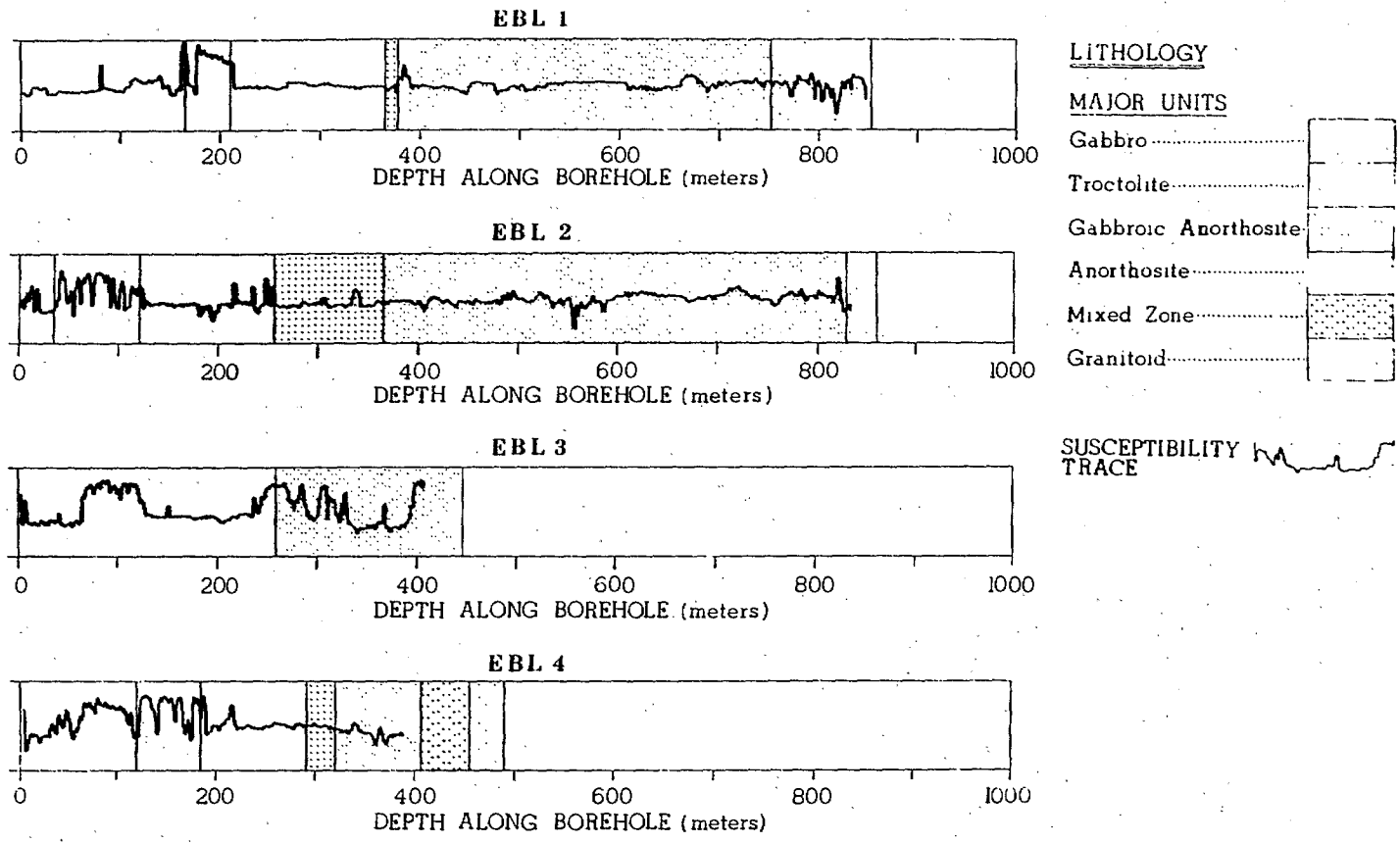


Figure 4.1.1 Lithology of Major Units and Susceptibility of EBL Drillholes.

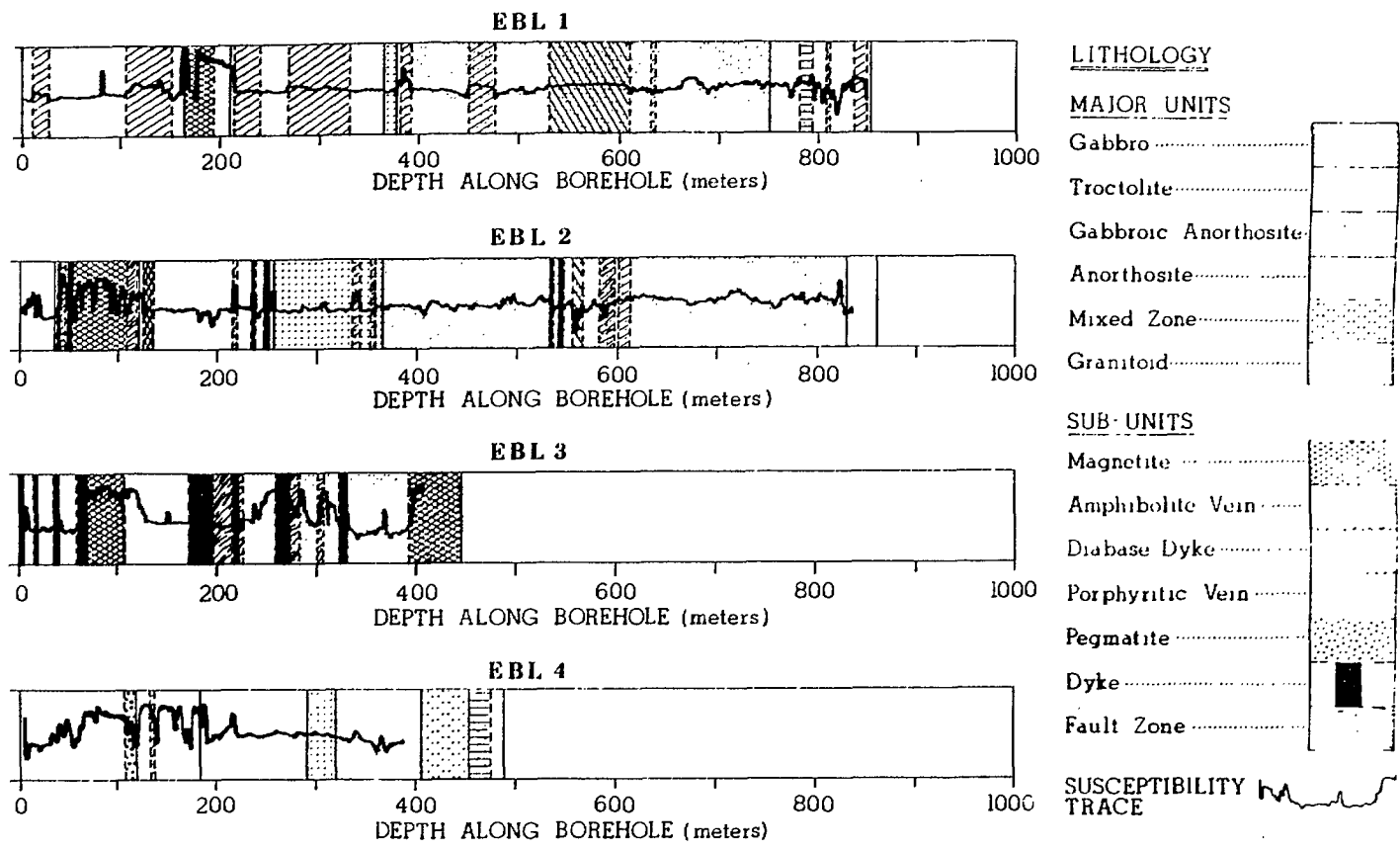
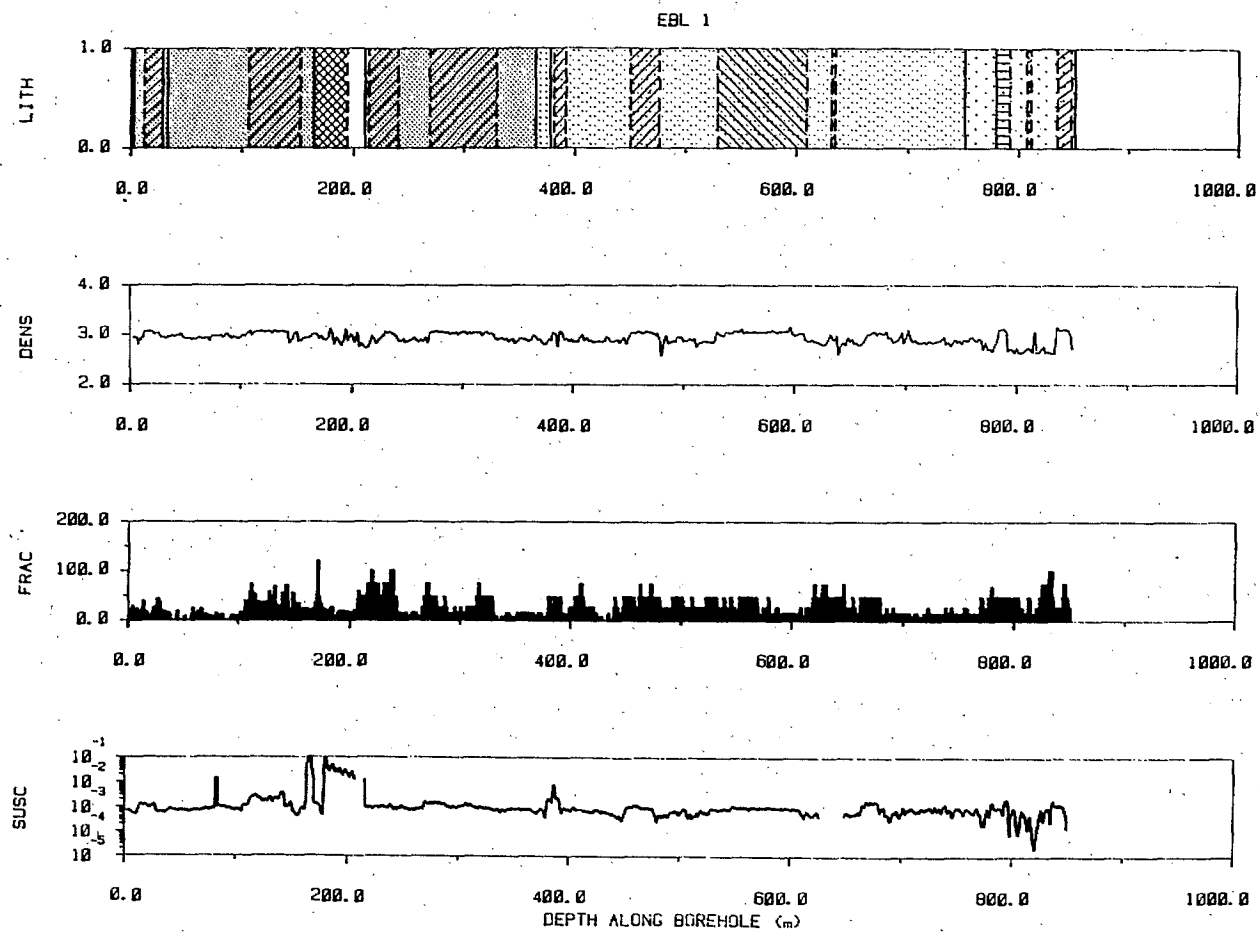


Figure 4.1.2 Lithology of Major and Sub-Units and Susceptibility of EBL Drillholes.



LITHOLOGY

MAJOR UNITS

- Gabbro
- Troctolite
- Gabbroic Anorthosite
- Anorthosite
- Mixed Zone
- Granitoid

SUB-UNITS

- Magnetite
- Amphibolite Vein
- Diabase Dyke
- Porphyritic Vein
- Pegmatite
- Dyke
- Fault Zone

Figure 4.1.3  
Lithology, Density, Fracture Frequency and Susceptibility of EBL-1.



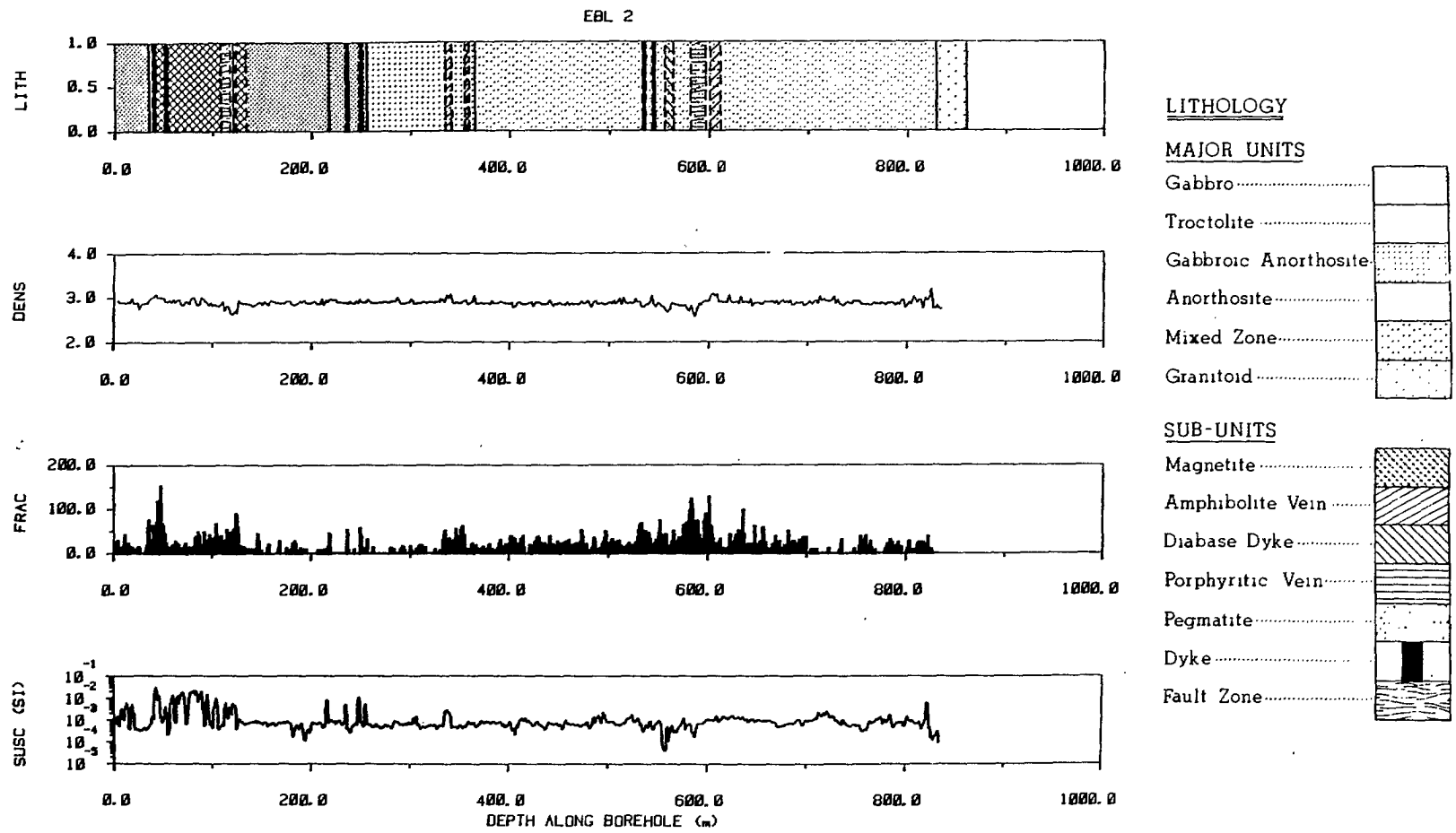
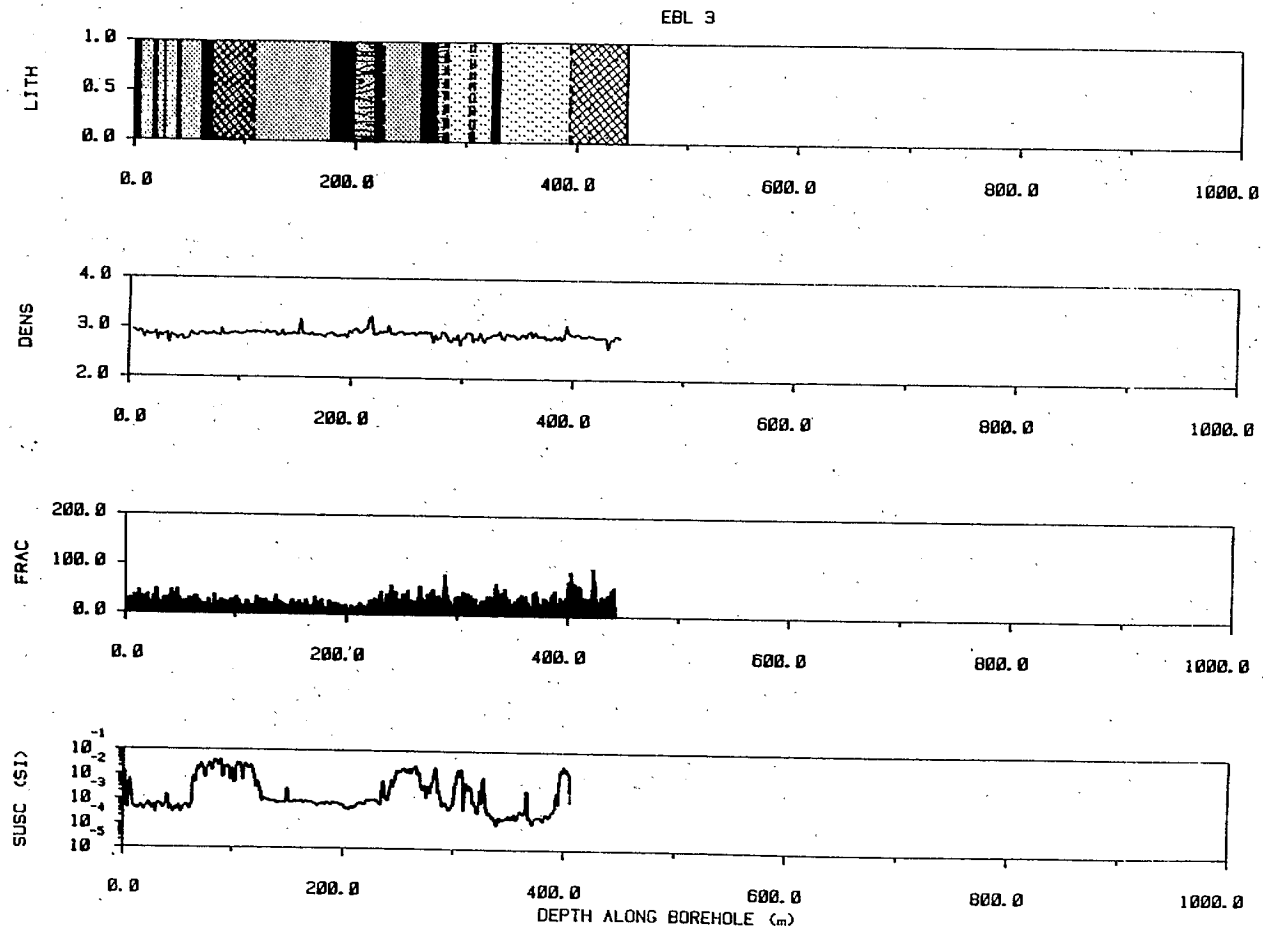


Figure 4.1.4  
Lithology, Density, Fracture Frequency and Susceptibility of EBL-2.



LITHOLOGY

MAJOR UNITS

- Gabbro
- Troctolite
- Gabbroic Anorthosite
- Anorthosite
- Mixed Zone
- Granitoid

SUB-UNITS

- Magnetite
- Amphibolite Vein
- Diabase Dyke
- Porphyritic Vein
- Pegmatite
- Dyke
- Fault Zone

Figure 4.1.5  
Lithology, Density, Fracture Frequency and Susceptibility of EBL-3.

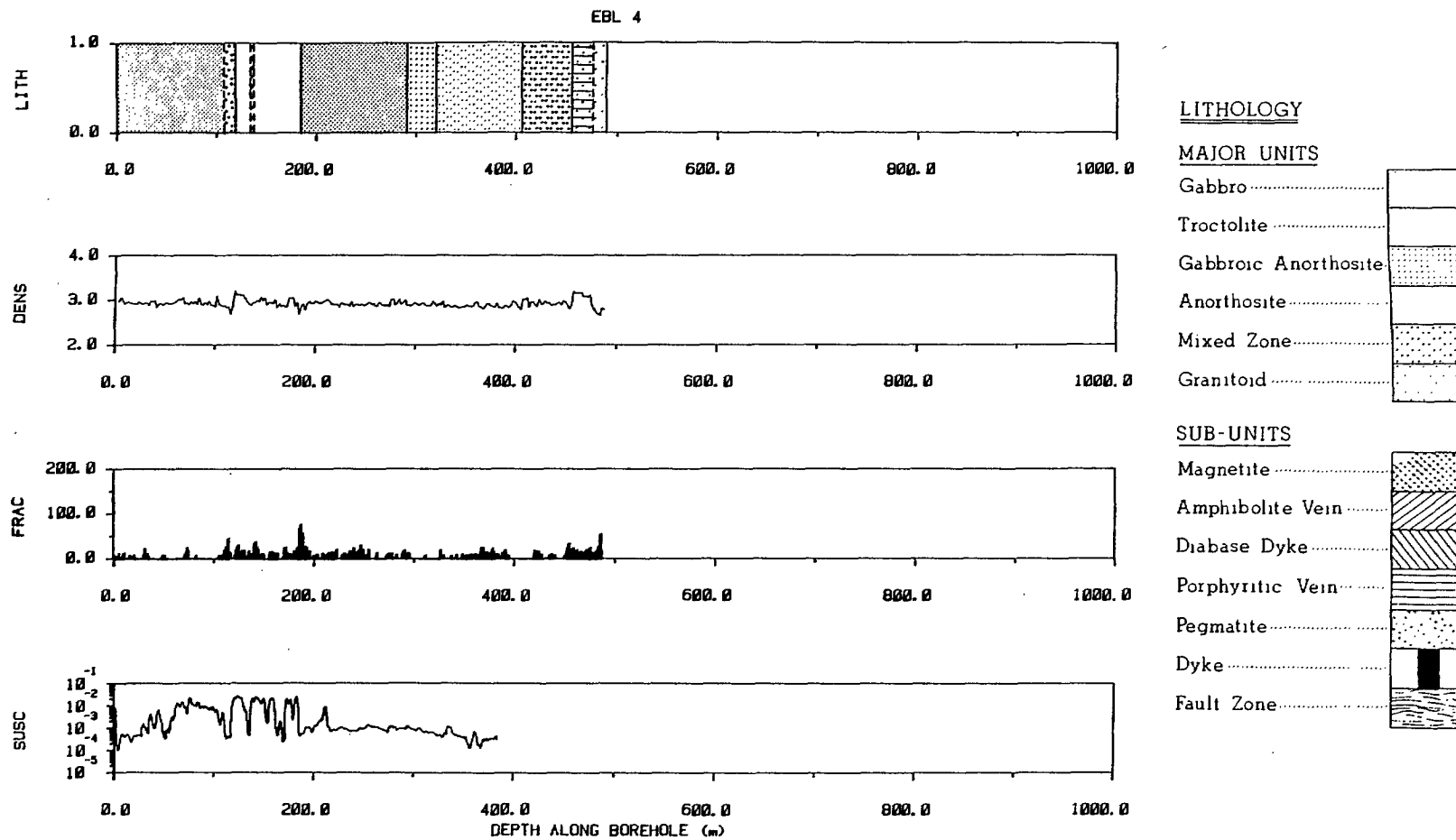


Figure 4.1.6  
Lithology, Density, Fracture Frequency and Susceptibility of EBL-4.

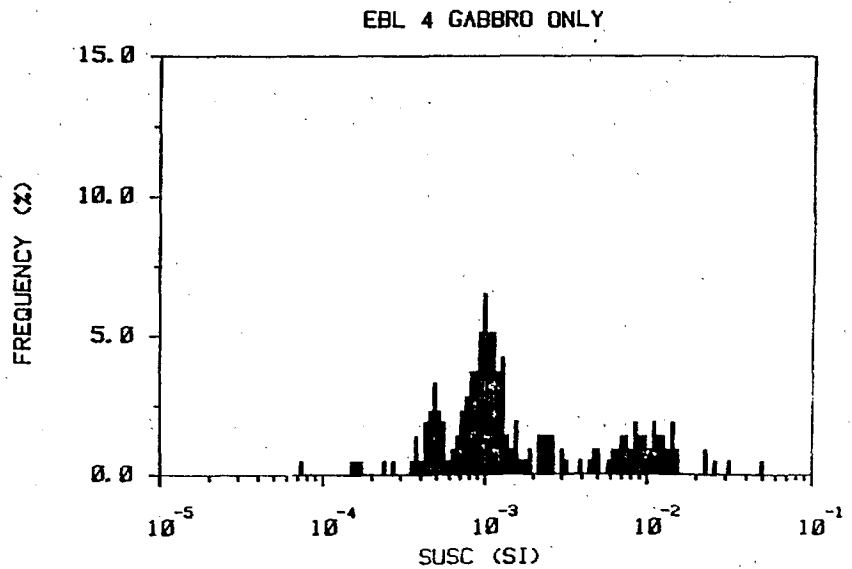
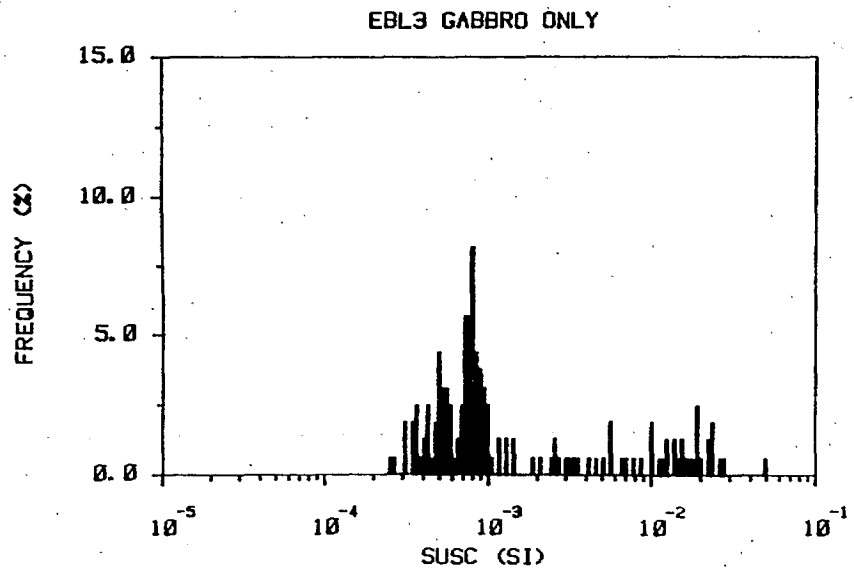
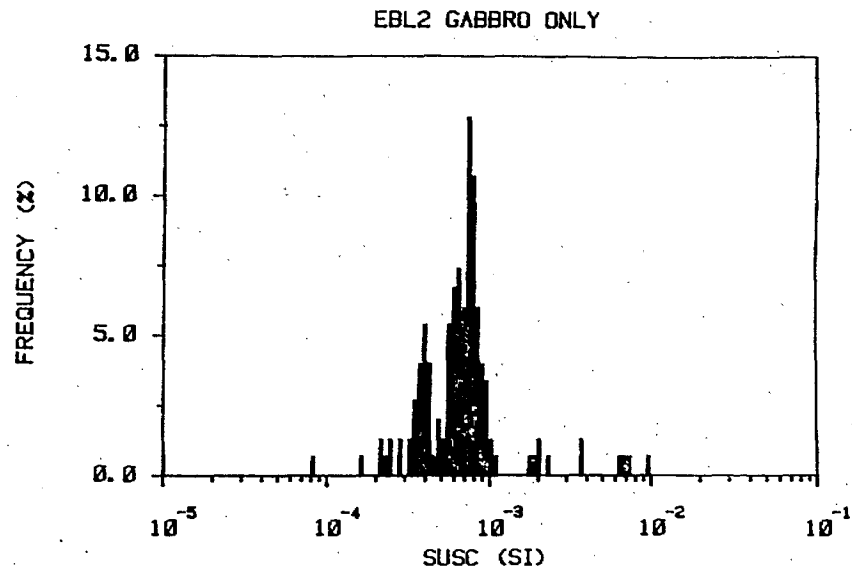
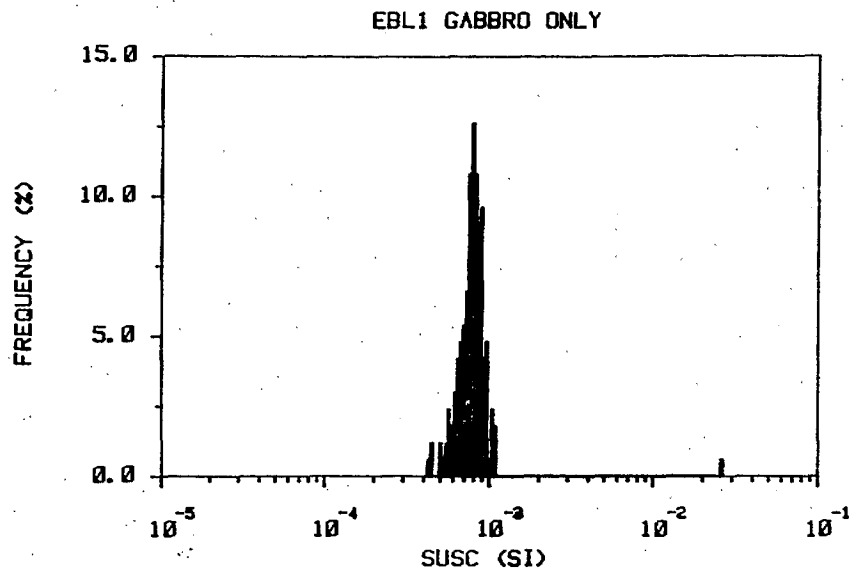


Figure 4.1.7 - Supportability Histograms for Gabbro Only

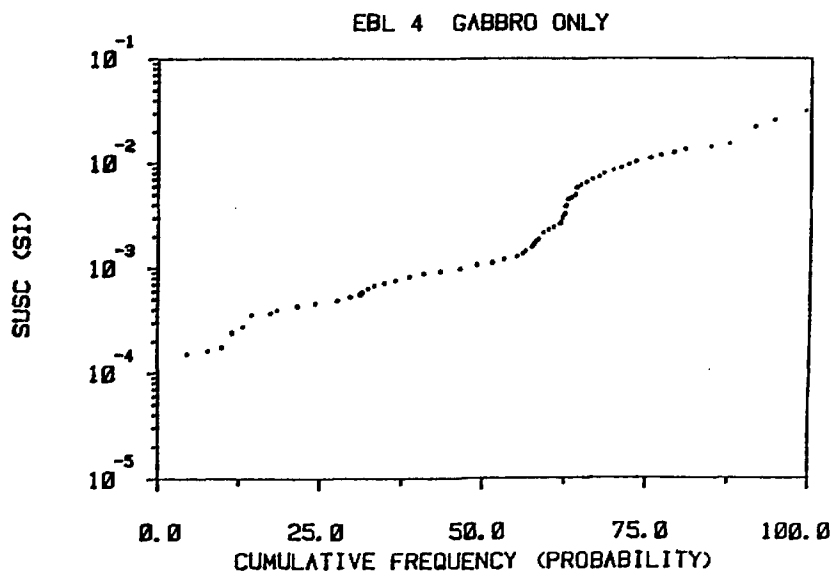
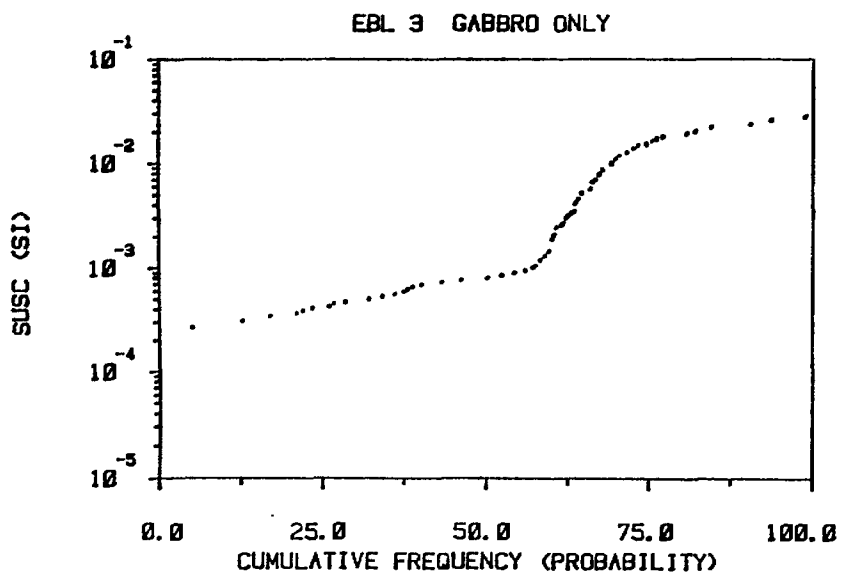
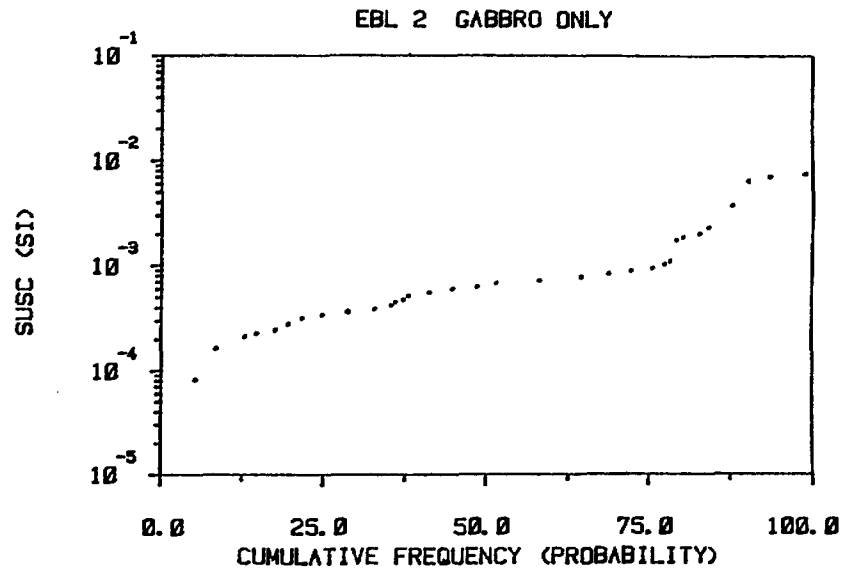
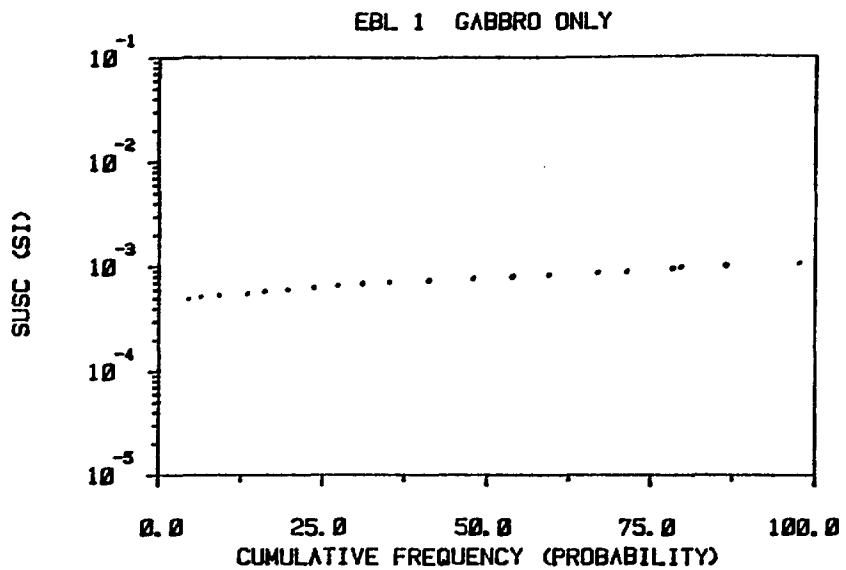


Figure 4.1.8 Cumulative Frequency Plots of Susceptibility of the Gabbroic Units.

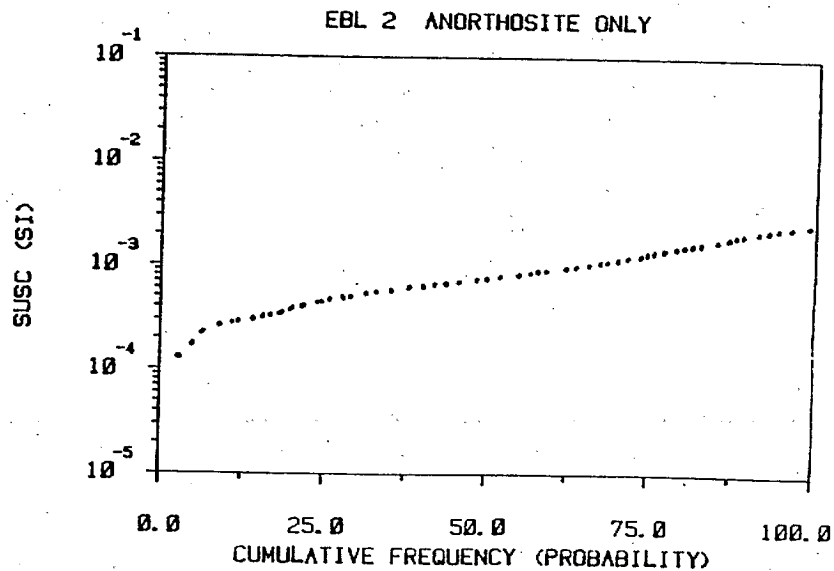
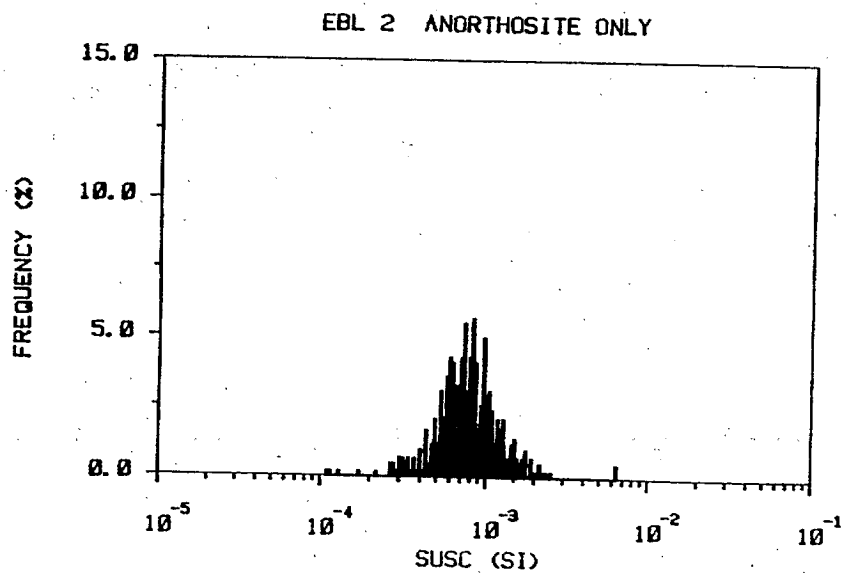
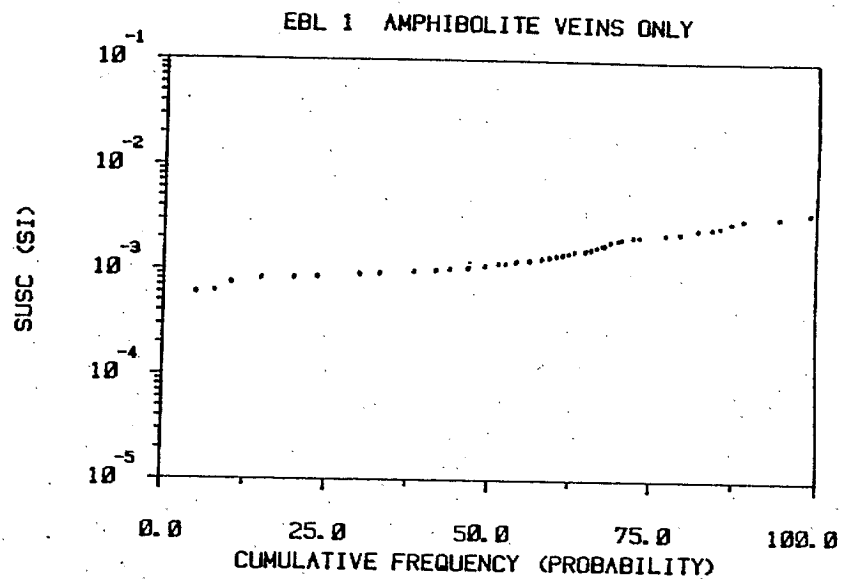
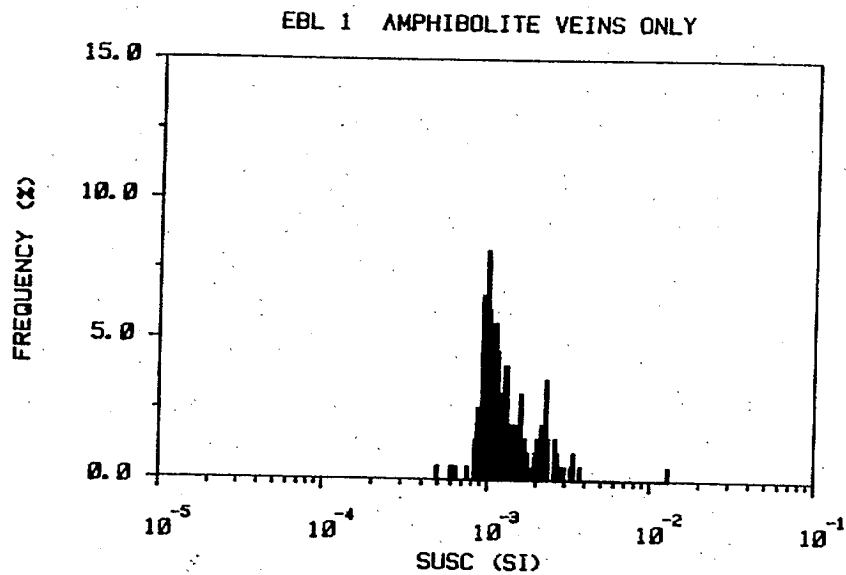


Figure 4.1.9 Susceptibility Histograms and Cumulative Plots for the

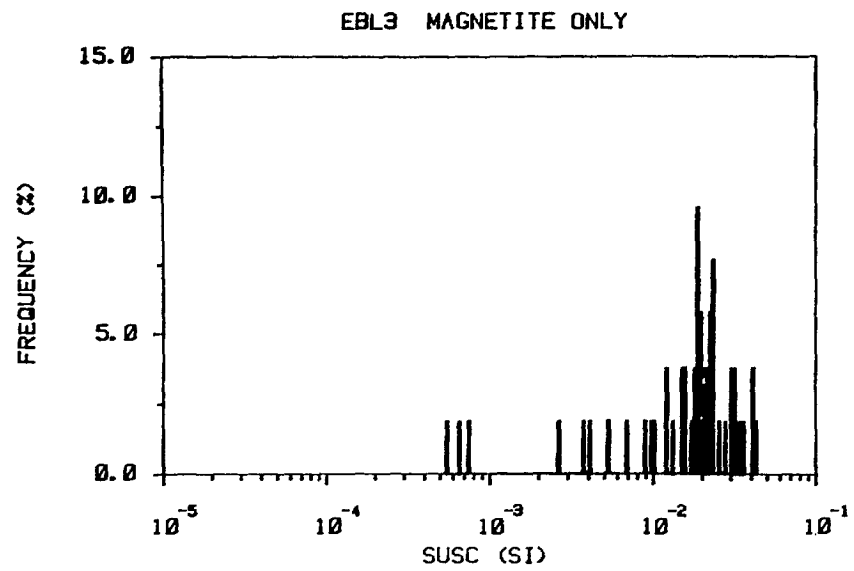
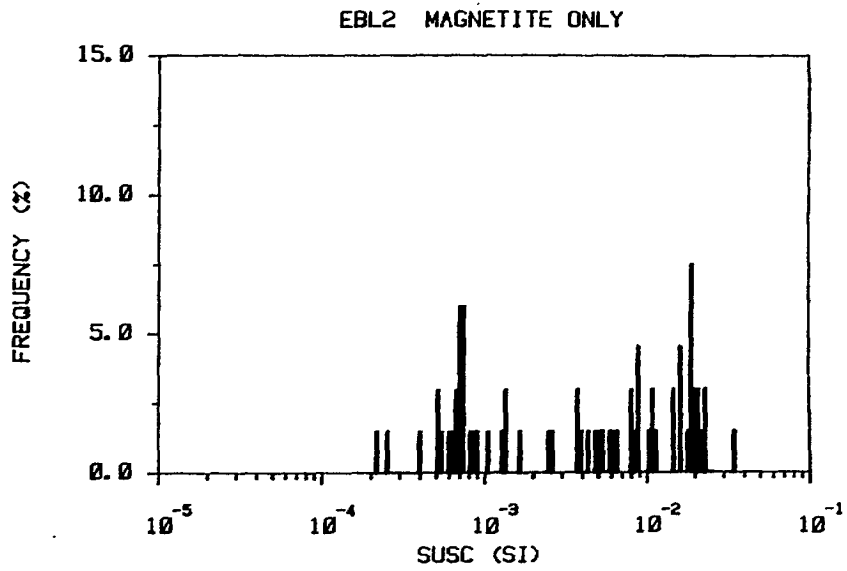
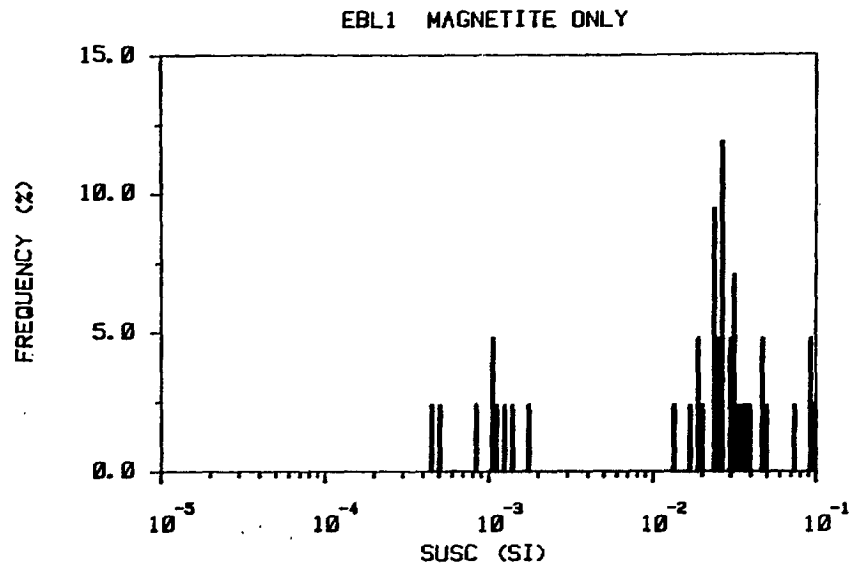


Figure 4.1.10  
Susceptibility Histograms of the  
Magnetite-Rich Units.

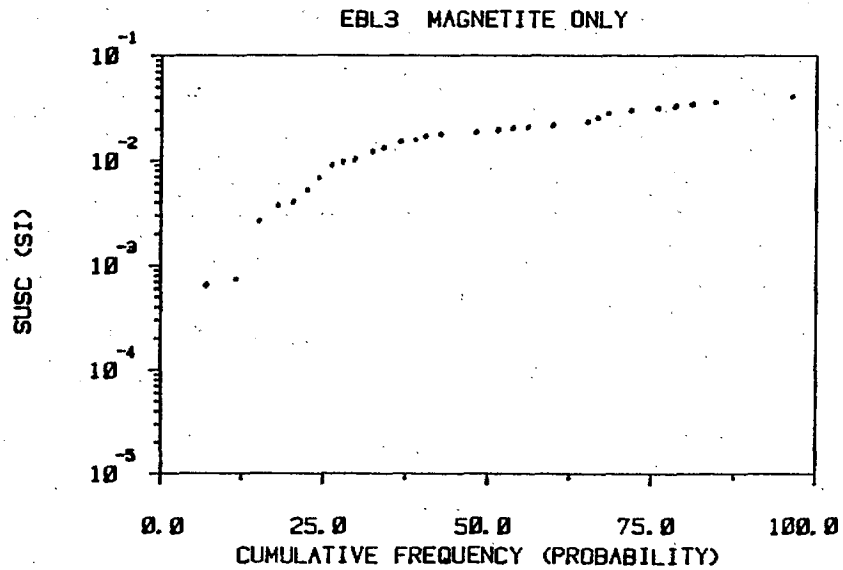
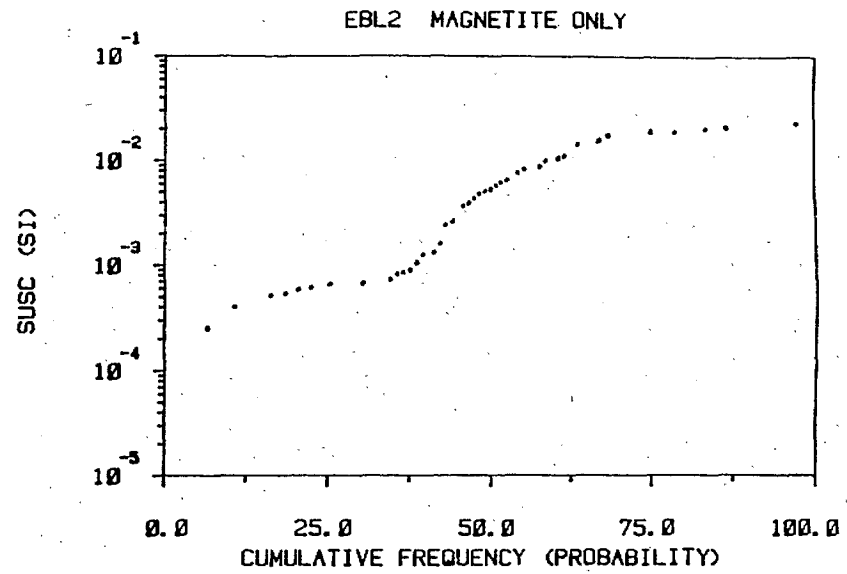
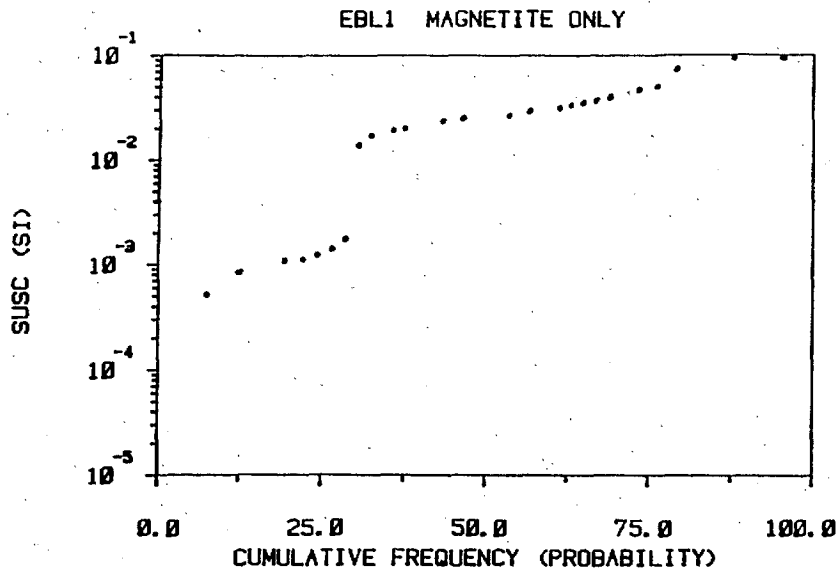


Figure 4.1.11  
Cumulative Frequency Plots of the  
Magnetite-Rich Units.



CHAPTER 5

EVALUATION OF ROCK PROPERTIES

A.G. Latham

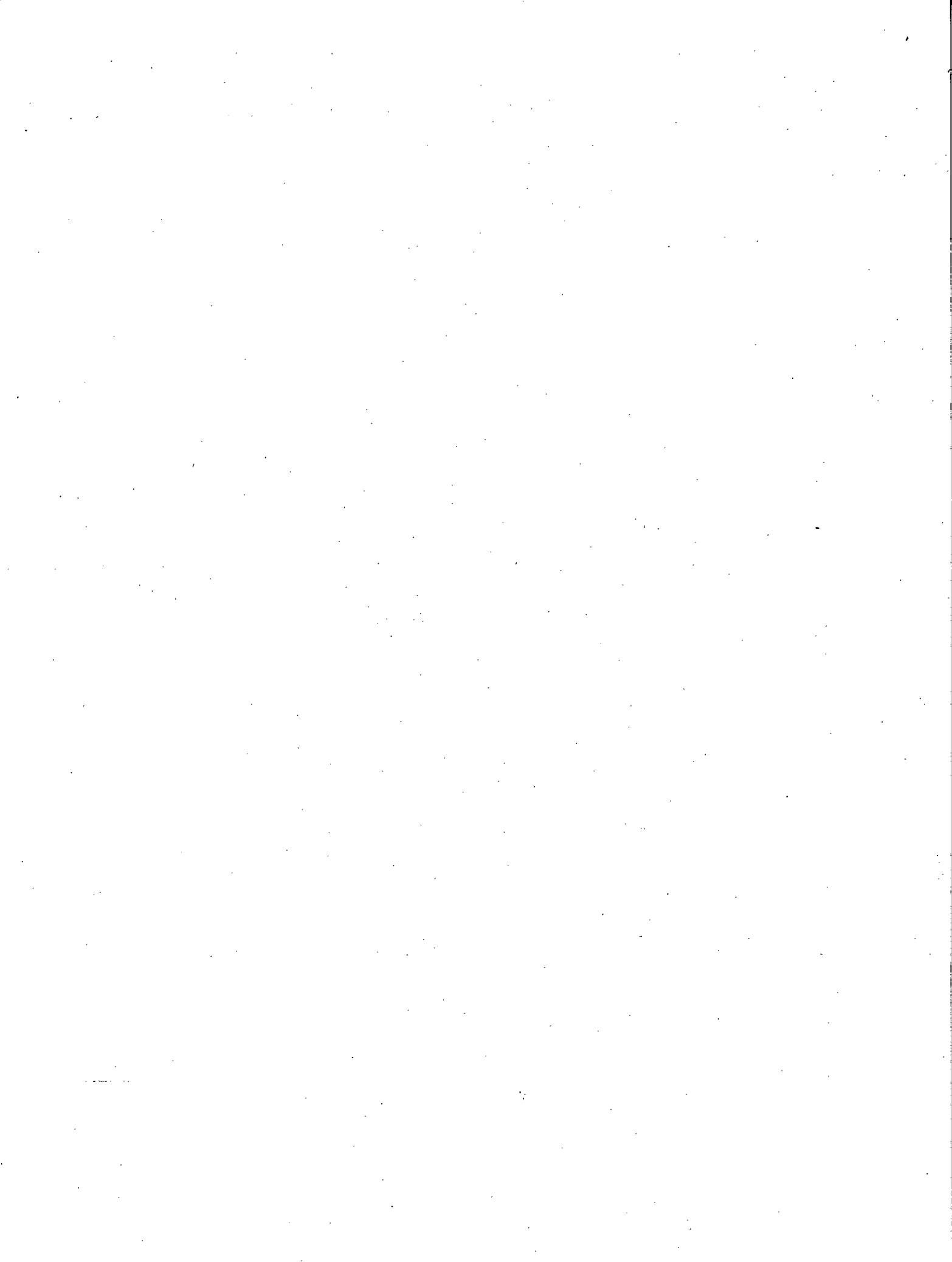
Geomagnetic Laboratory

Geological Survey of Canada

601 Booth Street

Ottawa, Ontario

K1A 0E8



## 5.1 Digest

The studies of this document relate to the various physical properties of the East Bull Lake gabbroic pluton. It should be noted that, except for the magnetic properties, all properties are evaluated for specimens of the rock matrix of hand-sample size and not to the macro-dimensions of the whole pluton.

The reasons for making the various rock-property studies were as follows:

- 1) The mechanical rock property data are needed in order to model the effects of the excavation on the surrounding vault surfaces, which includes an assessment of the rock competency, stress release, and of crack propagation.
- 2) Thermomechanical data are needed to model the effects of;
  - a) the conductivity of heat away from the vault;
  - b) the stress - temperature relationship; the differential thermal expansion of primary minerals and vein infillings;
  - c) the magnitude and configuration of thermo-hydraulic gradients.
- 3) Porosity data are required to model;
  - a) the rates of diffusion of released radionuclides;
  - b) to assess the relative contribution to radionuclide mobility of advection and diffusion;
  - c) to assess radionuclide bulk mechanical absorption (as opposed to chemical adsorption);
  - d) to assess temperature effects on diffusivity and advection;
  - e) to attempt to estimate the surface breakthrough times for the end-member case of the diffusion-only scenario.

Magnetic property measurements do not fall in the modelling categories annotated above, but qualify the fracture logs and aid in interpreting the history of the intrusion as a whole. The magnetic log thus represents a contribution to the geology of the whole pluton rather than to rock matrix properties per se, with the following important exception. It was noted (ch 4) that long-term alteration around fractures was much less than in either the URL or the ATK granites, and this is in accordance with the pore-structure data which showed that the permeability of the EBL rocks is indeed very low.

## 5.2 Distribution and Ranges of Values

Tables summarising the minimum, maximum and mean values are; for mechanical properties, tables 3.1.1 & 3.1.2, pp 35 and 36; porosity and permeability properties, table 3.2.1, p 53; and for thermal properties, table 3.3.1, p 67. For a more detailed analysis in which values for the individual lithological units are needed, the relevant chapter should be consulted.

The mechanical properties compare favourably with those of the Atikokan and Lac du Bonnet granites, though there is a greater variability due to the greater variation in EBL lithology (table 5.1). The mean value minus one standard deviation for the uniaxial compressive strength, is lowest for EBL, (152 MPa, of 186 for URL and 176 for ATK). (Values from Katsube and Hume (1987) and Robertson and Chernis (1987)).

Radionuclides in the rock migrate either by diffusion in the bulk rock (low flow regime) or by advection along fractures (relatively high flow regime). Therefore, the performance of the geological barrier must be assessed according to the relative contribution to migration of these two end-members. This study has highlighted the very low permeability of the bulk rock (ch 3.2), and the alteration zones around fractures was found to be much less than in the ATK or URL granites. In comparison with the granites, therefore, it may be concluded that:

- 1) If any water movement occurs in a geological barrier of this type, it will do so almost entirely by fractures - starting with the major fracture zones (least resistance) and later following the minor fractures (microcracks - most resistance).
- 2) There will be comparatively little mechanical absorption of radionuclides into the bulk of the rock, and consequently it may be expected that there will be relatively little chemical adsorption, as compared with the granites.
- 3) If there is any radionuclide adsorption it will be almost entirely on the walls of fractures, and on fracture-infilling minerals.

Thermal conductivity and thermal diffusivity affect the geometric configuration of isotherms and their rate of movement; that is, in the absence of water-bearing fractures, these factors determine how fast, and in which preferred directions, the residual heat is taken away from the vault. Figures 3.3.1 and 3.3.2 show that both conductivity and diffusivity are strongly dependent upon lithology.

### 5.3 Assessment of Values

First note that there are no thermomechanical data for any of the EBL units. At this stage therefore any modelling of the hot near-vault environment would have to assume values taken from elsewhere.

It may be assumed that many of the gabbro samples, tested for mechanical properties, contained healed micro-cracks. Also, since the gabbros are layered to varying extent, it may be that some mechanical properties are markedly anisotropic.

Note that uniaxial compressive strengths may vary by a factor of 3 (EBL 4), and are also likely to be anisotropic.

The three porosity parameters discussed in 3.2 do not include direct permeability measurements. However, the formation factor may be considered to be approximately the inverse of the permeability, and it is noted that both the mean formation factor ( $1.1 \times 10^5$ ) and the tortuosity (8.8) are considerably higher than for the Atikokan granite ( $3. \times 10^3$  and 2.7 respectively) (p.49). As stated in 3.2, "This implies that the diffusion rates will be much lower in these gabbros when compared with the granites."

In the case of the Lac du Bonnet granite, it was noted that samples taken from depth developed enhanced porosity and permeability because of stress release (ch. 5 of the URL Concept Assessment Document), and stress relief cracking was studied extensively (ch. 4). The analysis of the effects of stress relief on EBL rocks remains to be studied.

#### References

- Katsube, T.J. and Hume, J.P. 1987. Nuclear Fuel Waste Management Program, Concept Assessment Document: Geotechnical Studies at Whiteshell Research Area (RA-3): Rock Properties, for Atomic Energy of Canada Ltd. by Energy, Mines and Resources, 601 Booth Street, Ottawa, K1A 0E8, Canada.
- Robertson, B., and Chernis, P., 1987. Nuclear Fuel Waste Management Program, Concept Assessment Document: Geotechnical Studies at Atikokan Research Area (RA-4): Rock Properties, for Atomic Energy of Energy of Canada Ltd., by Energy, Mines and Resources, 601 Booth Street, Ottawa, K1A 0E8, Canada.

Table 5.1

Comparison of Mean Mechanical Properties of ATK, URL and EBL Samples

Area	Uniaxial Com. Strength M Pa	Young's Mod. G Pa	Poisson's Ratio
ATK <sup>1</sup>	212 ± 26	73.9 ± 15.2	0.26 ± 0.05
URL <sup>2</sup>	198 ± 12.6	66.0 ± 3.9	0.27 ± 0.04
EBL	202 ± 50	86.9 ± 14.9	0.27 ± 0.03

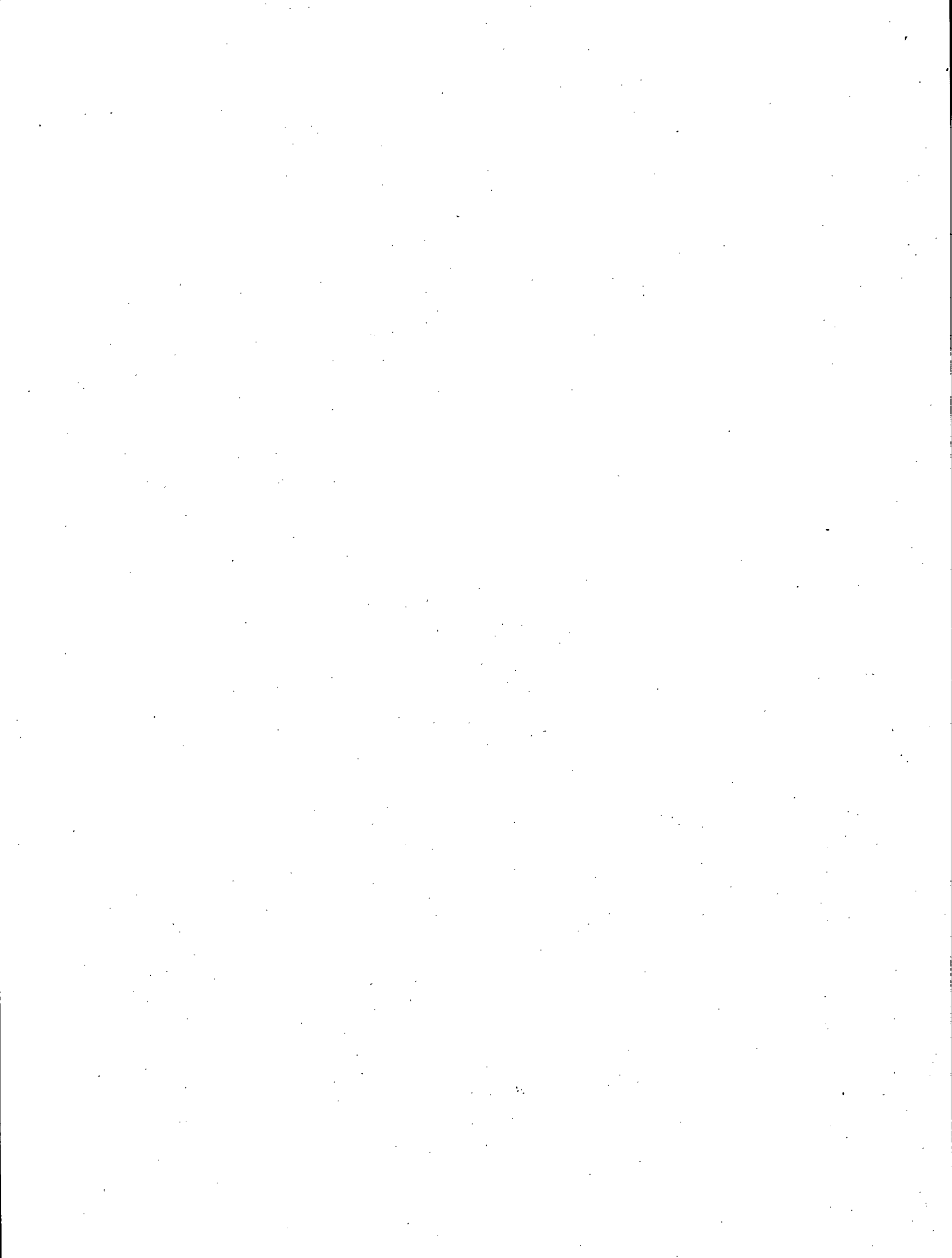
1. Katsube and Hume (1987).

2. Robertson and Chernis (1987).



CHAPTER 6

CONCLUSIONS AND RECOMMENDATIONS



6.1

CONCLUSIONS AND RECOMMENDATIONS

A.G. Latham  
Geomagnetic Laboratory  
Geological Survey of Canada  
601 Booth Street  
Ottawa, Ontario  
K1A 0E8

It, is pointed out again, that all rock property measurements have been carried out on laboratory samples of sizes not exceeding 20 cm. Therefore these studies have little to say about those greater scales where the effects of fractures are likely to be dominant. This means that, in the near vault environment, the mechanical data will be most useful when discussing stresses where fractures are absent or are small in all three dimensions. Similarly the porosity/permeability data is relevant to the case of radionuclide mobility by diffusion; it has less relevance to fracture conduit flow or to the possible evolution of convection cells which may be set up in fractures by existing topologically-driven or thermally-driven hydraulic gradients.

This report contains no data on mechanical properties at elevated temperatures ( $\approx 100^{\circ}\text{C}$ ), and there is no data for coefficients of thermal expansion for the different rock types or for any of the fracture infilling materials. Hence there is no firm data for assessing the effects of thermally-induced stresses in the near-vault environment. It is therefore not possible to assess how likely it will be, (1) that new fractures may be formed due to thermal effects, or (2) whether old sealed fractures may be reactivated due to the effects of any differential expansion between the country rock and its fracture-infilling material.

There is no elevated-temperature data on microcracks or on pore structure or other porosity-related parameters. Hence the ability to model the thermal effects on water permeability of fluid diffusivity in the vault environment will be impoverished to this extent.

HENCE THE CHIEF RECOMMENDATION OF THE REPORT IS THAT, FOR THE EAST BULL LAKE PLUTON, ALL ROCK PROPERTIES, INCLUDING THOSE OF MIXED COUNTRY ROCK AND FRACTURE INFILLINGS, NEED TO BE MEASURED AT ELEVATED TEMPERATURES IN ORDER THAT THE NEAR-VAULT ENVIRONMENT BE MODELLED MORE CONFIDENTLY.

